nature reviews earth & environment

https://doi.org/10.1038/s43017-023-00486-x

Review article

Check for updates

Mechanisms of tropical Pacific decadal variability

Antonietta Capotondi[1,2] ✉, Shayne McGregor[3,4], Michael J. McPhaden[5], Sophie Cravatte[6,7], Neil J. Holbrook[8,9], Yukiko Imada[10], Sara C. Sanchez[11], Janet Sprintall[12], Malte F. Stuecker[13,14], Caroline C. Ummenhofer[15,16], Mathias Zeller[17], Riccardo Farneti[18], Giorgio Graffino[19], Shijian Hu[20], Kristopher B. Karnauskas[1], Yu Kosaka[21], Fred Kucharski[18], Michael Mayer[22,23], Bo Qiu[13], Agus Santoso[16,24], Andréa S. Taschetto[16,24], Fan Wang[20], Xuebin Zhang[25], Ryan M. Holmes[26], Jing-Jia Luo[27], Nicola Maher[1,11,28,29], Cristian Martinez-Villalobos[30,31], Gerald A. Meehl[32], Rajashree Naha[3], Niklas Schneider[13,14], Samantha Stevenson[33], Arnold Sullivan[34], Peter van Rensch[3] & Tongtong Xu[1,2]

Abstract

Naturally occurring tropical Pacific variations at timescales of 7–70 years — tropical Pacific decadal variability (TPDV) — describe basin-scale sea surface temperature (SST), sea-level pressure and heat content anomalies. Several mechanisms are proposed to explain TPDV, which can originate through oceanic processes, atmospheric processes or as an El Niño/Southern Oscillation (ENSO) residual. In this Review, we synthesize knowledge of these mechanisms, their characteristics and contribution to TPDV. Oceanic processes include off-equatorial Rossby waves, which mediate oceanic adjustment and contribute to variations in equatorial thermocline depth and SST; variations in the strength of the shallow upper-ocean overturning circulation, which exhibit a large anti-correlation with equatorial Pacific SST at interannual and decadal timescales; and the propagation of salinity-compensated temperature (spiciness) anomalies from the subtropics to the equatorial thermocline. Atmospheric processes include midlatitude internal variability leading to tropical and subtropical wind anomalies, which result in equatorial SST anomalies and feedbacks that enhance persistence; and atmospheric teleconnections from Atlantic and Indian Ocean SST variability, which induce winds conducive to decadal anomalies of the opposite sign in the Pacific. Although uncertain, the tropical adjustment through Rossby wave activity is likely a dominant mechanism. A deeper understanding of the origin and spectral characteristics of TPDV-related winds is a key priority.

Sections

A full list of affiliations appears at the end of the paper. ✉e-mail: antonietta.capotondi@noaa.gov

Introduction

The tropical Pacific atmosphere–ocean system (Box 1) exhibits variability over a broad range of timescales: the El Niño/Southern Oscillation (ENSO) dominates at interannual timescales (~2–7 years), and the trend from anthropogenic forcing at centennial. In the intermediate range, natural (internal) variations occur at quasidecadal and multidecadal timescales (7–70 years)[1], encompassing the broadly termed tropical Pacific decadal variability (TPDV). TPDV represents the tropical expression of the Pacific decadal oscillation[2] in the North Pacific and the interdecadal Pacific oscillation[3] over the entire Pacific basin. Its positive phase is characterized by warm sea surface temperature anomalies (SSTAs) in the tropical Pacific and along the western coasts of the Americas, and by negative anomalies in the central and western midlatitudes of both hemispheres; the negative phase exhibits anomalies of the opposite sign.

TPDV has important climatic relevance. For example, it modulates ENSO characteristics[4,5] and some of its global impacts, including climatic variations over Antarctica[6], Australian monsoon variability[7] and temperature and precipitation over the western USA[8], making prediction of TPDV phases societally critical. TPDV is further linked to the rate of change of globally averaged surface temperature[9,10] as demonstrated by the decrease in globally averaged surface temperature trend during the cold TPDV phase in the first decade of the 2000s. Accordingly, understanding TPDV is integral to robustly separate the forced climate response from internally generated climate variability and thereby produce reliable projections of tropical Pacific and global climate[9]. Yet, some models appear to underestimate internally generated decadal variations[11–13] and might incorrectly simulate externally forced trends, introducing uncertainty in attribution analyses[14–17]. This ambiguity highlights the importance of a deepened understanding of internal low-frequency variability and prediction of decadal epochs in the tropical Pacific.

However, TPDV predictability currently remains elusive, largely related to complicated, and often competing, underlying mechanisms. For instance, TPDV could result as a residual of interannual ENSO variability[18], or result from equatorial upwelling of subtropical temperature anomalies from the pycnocline (the $\bar{v}T'$ hypothesis, in which $\bar{v}$ indicates the time mean circulation and T' is the temperature anomaly)[19], or changes in equatorial upwelling itself (the $v'\overline{T}$ hypothesis, in which v' indicates the circulation anomaly and $\overline{T}$ is the time mean temperature)[20]. Moreover, these oceanic mechanisms could be driven by atmospheric forcing resulting from processes in the extratropical Pacific[21], responding to equatorial SSTAs[22] or arising from interactions with the Atlantic and Indian Oceans[23,24]. Yet, no consensus exists on the effectiveness and relative importance of these processes.

In this Review, we critically elucidate the nature and relative importance of the mechanisms driving TPDV using evidence from observations, ocean reanalyses, dynamical models and paleoclimate proxies. We begin by describing salient features of TPDV in the context of the phase transition that occurred in the late 1990s. We follow with discussion of the leading oceanic and atmospheric processes relevant for TPDV, including as an ENSO residual; the $\bar{v}T'$ hypothesis; the $v'\overline{T}$ hypothesis; and extratropical and tropical forcing and influences from other ocean basins. We end with recommendations for future research. Relative to other reviews that have considered internal and anthropogenically forced low-frequency variability[18], focus here is on internal decadal variations.

Observed tropical Pacific decadal changes

Before reviewing the mechanisms, it is important to identify the key oceanic and atmospheric changes that accompany decadal phase transitions in the tropical Pacific. A comparison of 1984–1999 (a generally positive TPDV) with 1999–2014 (a generally negative TPDV) typifies these transitions (Fig. 1); changes during negative-to-positive decadal transitions largely mirror those shown and described[25,26].

The phase change reflects a marked shift in SSTs, characterized by cold conditions in the equatorial Pacific and warm anomalies in the central and western midlatitudes (Fig. 1a, shading). This SST difference pattern is similar to that obtained through a statistical definition of TPDV (Fig. 1a, contours): the linear regression of SSTAs on the TPDV index, the latter defined as the principal component of 7–70 years band-pass-filtered SSTAs in the tropical Pacific (25° S–25° N). The spatial structure of the tropical decadal SST pattern is 'ENSO-like'; the overarching characteristics are similar, but SST anomalies are broader in the meridional extent and the largest equatorial variability is shifted further west than the interannual ENSO variance[18,27].

Such large-scale SST changes are accompanied by corresponding changes in the atmosphere that, in turn, influence the ocean. Specifically, positive sea-level pressure (SLP) anomalies in the extratropics (Fig. 1b, shading) drive enhancement of the easterly trade winds (Fig. 1b, vectors), in turn, causing heat content reorganization[11,28–30]. Positive sea surface height (SSH) differences, indicative of a deeper thermocline, are found in the western tropical Pacific (Fig. 1c), with increased heat content (Fig. 1e, shading) at the depth of the mean thermocline (Fig. 1e, contours), all largely associated with westward-propagating Rossby waves[26]. By contrast, negative SSH differences (shallower thermocline) are found in the central and eastern Pacific (Fig. 1c), with decreased heat content in the upper ocean east of the dateline (Fig. 1f, shading). Positive SSH anomalies are also present in the Indonesian Seas and eastern Indian Ocean[31,32], suggesting a transfer of heat from the Pacific to the Indian Ocean, likely associated with wind impacts on the Indonesian Throughflow (ITF)[16,33,34].

The mechanisms proposed for such TPDV are multifaceted. The presence of trends[11], particularly in SSH across the western Pacific, Indonesian Seas and eastern Indian Ocean[35–37] (Fig. 1c,d), adds further challenge in separating natural and anthropogenic forcings and in determining the relative importance of various TPDV processes. The key mechanisms are now discussed, starting with the possibility that TPDV arises as a residual of interannual ENSO variations.

TPDV as an ENSO residual

Since the tropical Pacific climate is dominated by interannual ENSO variations, a plausible hypothesis is that TPDV arises as a residual of ENSO. Indeed, the ENSO-like TPDV spatial pattern[27] can be reconstructed from decadal averages of evolving ENSO patterns, from their developing to decaying phases and from random event-to-event variations of those patterns[18,38]. In addition, uneven numbers of warm (El Niño) or cold (La Niña) events randomly occur during different decadal epochs (Fig. 2a), resulting in El Niño-like or La Niña-like decadal conditions. The location of SSTA during these uneven events (whether anomalies are centred in the eastern or central Pacific)[39] (Fig. 2a) might also contribute to low-frequency background changes[40].

Similar to the influence of stochastic subseasonal disturbances on the development of El Niño[41,42], ENSO events could also act as triggers for TPDV phase transitions. Specifically, some ENSO events could induce off-equatorial wind stress curl anomalies responsible for the excitation of oceanic Rossby waves and for the discharging–recharging of the anomalous heat content in the western Pacific[43] (Fig. 1c), causing a TPDV transition. These heat content anomalies are an important necessary condition for ENSO-induced changes in TPDV phase[43,44].

Box 1

Mean ocean and atmospheric circulations in the tropical Pacific

The equatorial Pacific Ocean is often described as a system with a warmer and dynamically active upper layer and a colder and more quiescent bottom layer (see the figure, bottom). These two layers are separated by a region of sharp vertical density and temperature gradients, known as the pycnocline and thermocline, and are overlaid by a near-surface frictional layer — the Ekman layer.

The pycnocline links subtropical regions to the equator: subtropical waters can penetrate into the ocean interior at the latitudes where surfaces of constant density (isopycnals) meet the near-surface layer and then flow equatorward along those isopycnals. At the equator, these waters are brought to the upper layers by the upward vertical velocity (upwelling), and returned to higher latitudes by the flow in the surface Ekman layer (see the figure, bottom, black solid arrows), creating shallow overturning circulations in both hemispheres termed subtropical cells[20]. Warm tropical sea surface temperatures drive the atmospheric Hadley cells (see the figure, top), with air rising near the equator, flowing poleward in the troposphere at 10–15 km above the surface, and descending in the subtropics, with an equatorward return flow near the surface that is deflected westward because of the rotation of the Earth, creating the easterly trade winds.

The tropical Pacific Ocean circulation also exhibits a rich system of zonal currents (see the figure, top), with both westward and eastward flowing currents. The most noteworthy of these is the equatorial undercurrent (EUC), a strong eastward flowing jet centred on the equator with a core in the pycnocline (see the figure, bottom). The zonal slope of the pycnocline — deeper in the west and shallower in the east — is in balance with the easterly equatorial trade winds and provides the pressure gradients that drive the EUC. The trade winds are the surface branch of the zonal atmospheric Walker circulation, consisting of an ascending branch over the warm waters of the western equatorial Pacific 'Warm Pool' and a descending branch in the colder and drier eastern equatorial Pacific 'Cold Tongue' (see the figure, top).

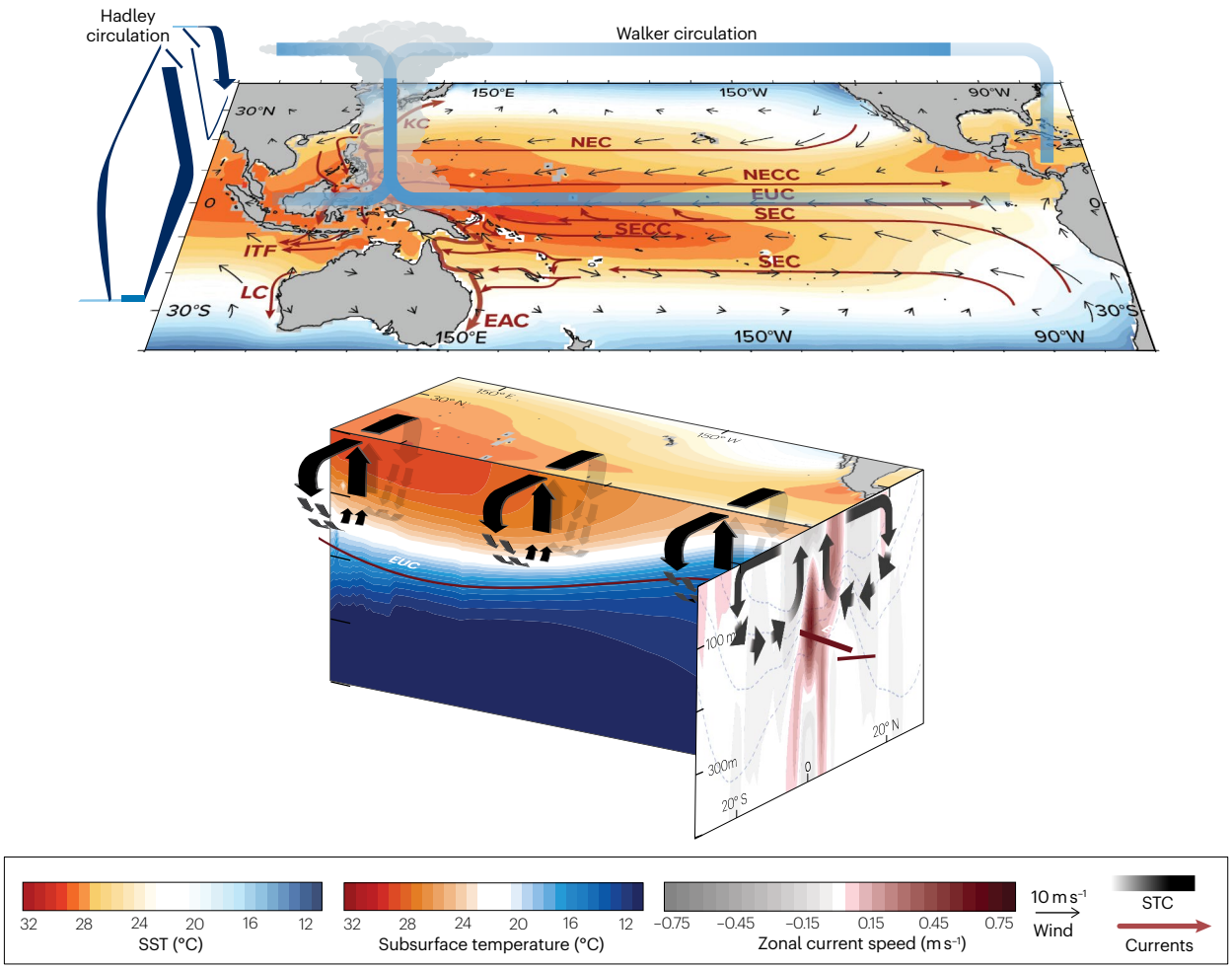

(continued from previous page)

The interior wind-driven zonal circulation is connected in the western Pacific to the equatorward flowing low-latitude western boundary currents, which are an important conduit for the redistribution of subtropical water to the western equatorial Pacific[170] and then into the tropical current system, including the EUC and the Indonesian Throughflow.

EAC, East Australian current; ITF, Indonesian throughflow; KC, Kuroshio current; LC, Leeuwin current; NEC, North equatorial current; NECC, North equatorial countercurrent; SEC, South equatorial current; SECC, South equatorial countercurrent; SST, sea surface temperature; STC, subtropical cell.

Additionally, oceanic nonlinearities associated with strong El Niño events during a positive TPDV phase could induce strong negative feedbacks and cause a transition to negative TPDV[45].

The interpretation of TPDV as an ENSO residual also involves subsurface anomalies. Western Pacific heat content exhibits a decadal modulation, with reduced heat content during periods of positive TPDV (such as 1976–1999) (Fig. 2b,d) and enhanced heat content during negative TPDV (such as 1999–2014) (Fig. 2b,d). These low-frequency variations are punctuated by the heat content changes associated with the recharge–discharge activity of individual ENSO events (Fig. 2b), which are the dominant signal in the eastern Pacific (Fig. 2c). The decadal modulation of tropical Pacific heat content could thus be interpreted as the low-frequency envelope of interannual ENSO variations.

However, ENSO characteristics also depend on the mean state[46,47]. Indeed, the warm phase of TPDV, characterized by weaker trade winds and a deeper thermocline in the eastern equatorial Pacific, favours more frequent and stronger eastern Pacific El Niño events (Fig. 2a), whereas negative TPDV phases are characterized by weaker central Pacific El Niño events (Fig. 2a). The mean state influence on ENSO was also highlighted by dynamic model prediction experiments in which the ENSO evolution and predictive skill[48,49] were highly dependent on the initial background conditions. The decadal modulation of ENSO, as captured in climate models by the second empirical orthogonal function of decadal SSTAs[4,50,51], is significantly lag-correlated with TPDV[51], with a large intermodel dependence[50]. ENSO decadal modulation appears to lead the opposite phase of TPDV by about 2 years, suggesting its possible role as precursor of TPDV phase transitions[51]. However, TPDV also leads the same phase of ENSO decadal modulation by 2 years with a higher correlation[51], indicating that ENSO modulation by TPDV might be more prominent than the influence of ENSO activity on TPDV. Additionally, empirical models trained on observations indicate that tropical–extratropical interactions are key to the existence of TPDV, implying that TPDV cannot simply arise from processes occurring within the tropics as in the case of ENSO residuals[52].

The $\bar{v}T'$ hypothesis and wave processes

In addition to the possibility of being an ENSO residual, equatorward advection of temperature anomalies within the pycnocline (the $\bar{v}T'$ hypothesis) has been put forward as a driver of TPDV[19] (Fig. 3a). Two mechanisms by which subtropical signals reach the equator have been proposed: spiciness anomalies advected as passive tracer by the mean circulation and non-compensated temperature anomalies propagating as planetary (Rossby) waves, as discussed now.

Advection of spiciness anomalies

Spiciness anomalies describe temperature anomalies with a density compensating salinity signal[53]; they do not affect density and propagate along isopycnals as a passive tracer[54] (Fig. 3a). These warm-salty or cold-fresh anomalies are predominantly generated in the eastern subtropical Pacific[55,56] through shifts in spiciness gradients induced by wind-forced anomalous ocean currents[54], or buoyancy-forced penetrative mixing[56]. Spiciness anomalies are subsequently advected by the subsurface branches of the subtropical cells (STCs) towards the equator. Despite some decay[57–59], observations support the generation and propagation of spiciness anomalies from the eastern subtropics to the western tropical Pacific. However, whether these anomalies are advected all the way to the equator is much less clear, and the feasibility of a western boundary pathway is uncertain owing to the complexity of low-latitude western boundary currents (LLWBCs) and high mixing and water mass transformation[60]. A Lagrangian modelling approach indicates that spiciness anomalies reach the eastern equatorial band[61], with clear dominance of southern hemisphere pathways. At large spatial scales, theoretical arguments suggest that pycnocline advection might result in a frequency spectrum of spiciness anomalies reaching the equator with enhanced power in the decadal range[62].

Such decadal-scale spiciness anomalies might drive TPDV. Specifically, coupled model experiments suggest that equatorward-advected spiciness anomalies are upwelled to the surface where they rearrange equatorial SSTs, winds and the slope of the pycnocline[63], in turn, inducing atmospherically forced off-equatorial spiciness anomalies of opposite sign, resulting in a 10-year cycle[54,63]. A heat budget analysis of the modelled equatorial Pacific mixed layer further confirms this influence of spiciness anomalies on TPDV[59], although with a small magnitude relative to other heat budget terms leaving the efficiency of this mechanism unclear.

Wave propagation of non-compensated temperature anomalies

An alternative mechanism within the $\bar{v}T'$ hypothesis is the propagation of temperature anomalies via Rossby waves. Oceanic Rossby waves cause isopycnal displacements that appear as temperature anomalies over time-mean isopycnal surfaces. These anomalies reach the equatorial thermocline via the western boundary and propagate eastward along the equator as equatorial Kelvin waves, altering equatorial SSTs. As such, Rossby wave activity has been related to decadal subsurface temperature anomalies in the tropical Pacific with maxima around 10°–15° N and 10°–14° S (refs. 26,64–68) (Fig. 1c).

However, the origin of the decadal timescale remains unclear given that the Rossby wave transit time at key latitudes (10°–15° N and 10°–14° S) is only 2–3 years. Several hypotheses have been put forward as an explanation. First, the latitudes of Rossby wave maxima coincide with areas of high zonal coherence of the wind forcing, which might be efficient in exciting large amplitude waves at decadal timescales[65]. Second, these latitudes coincide with the equatorward boundaries of the subtropical gyres, where instability processes can energize

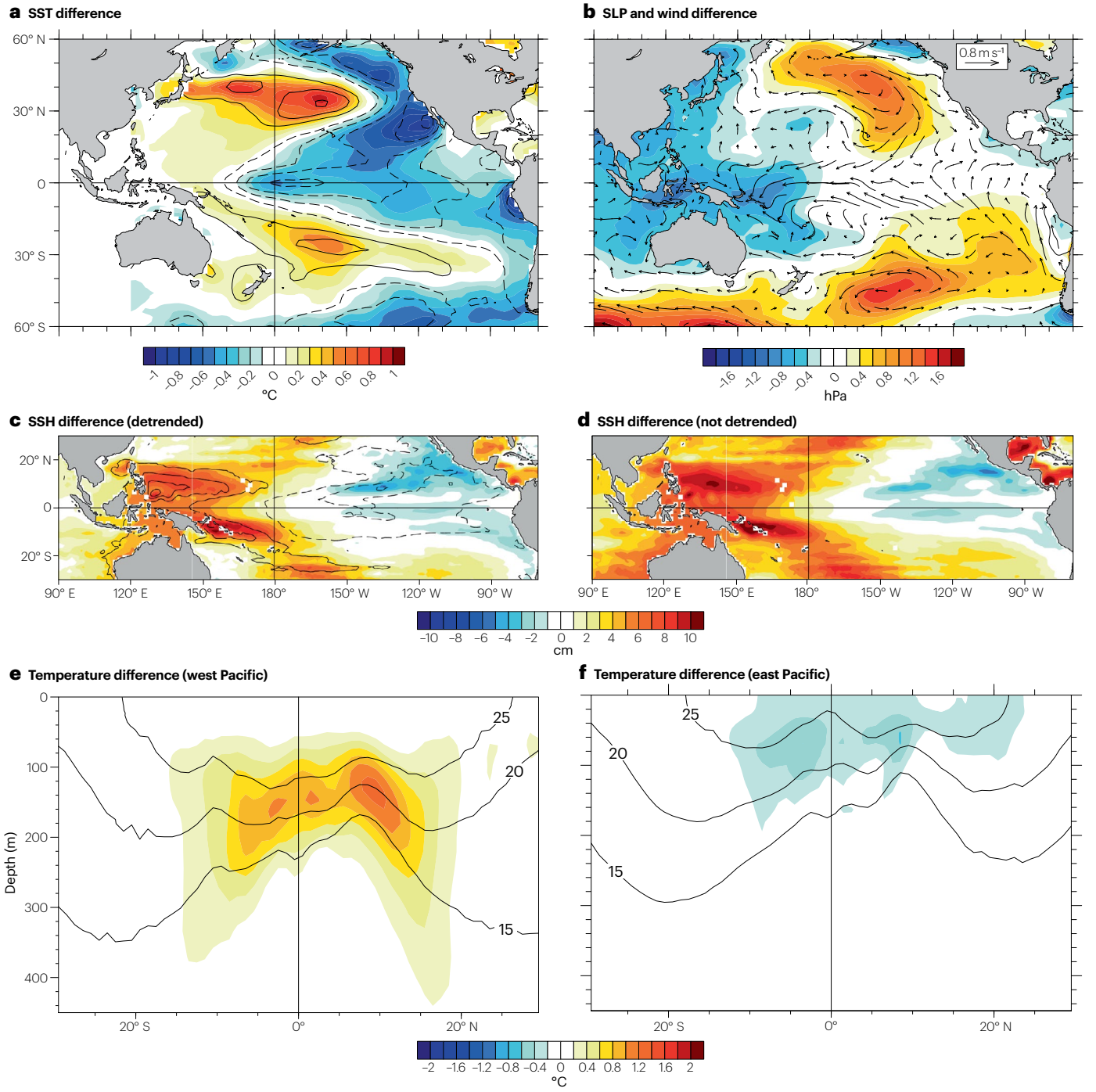

Fig. 1 | Observed Pacific decadal changes. a, The difference of linearly detrended sea surface temperature (SST) anomalies[161] (shading) and decadal SST anomalies regressed onto the tropical Pacific decadal variability (TPDV) index (contours). **b**, Differences of linearly detrended sea-level pressure (SLP; shading) and vector wind anomalies[162] (arrows). **c**, Differences of linearly detrended sea surface height (SSH) anomalies[163] (shading) and decadal SSH anomalies regressed on the TPDV index (contours). **d**, Differences of un-detrended SSH anomalies[163]. **e**, Differences of detrended temperature anomalies zonally averaged between the western ocean boundary and the dateline; contours indicate the time mean (1979–2017) 15, 20 and 25 °C isotherms. **f**, As in panel **e**, but for temperature values averaged from the dateline to the eastern ocean boundary. In all panels, differences represent 1999–2014 minus 1984–1999, and regressions are calculated over 1958–2020. In panels **a** and **c**, solid contours represent positive anomalies and dashed contours represent negative anomalies, drawn at 0.1 °C intervals for SST and 1 cm for SSH. TPDV is associated with basin-wide SST, SLP and wind anomalies and involves a reorganization of heat content in the tropics.

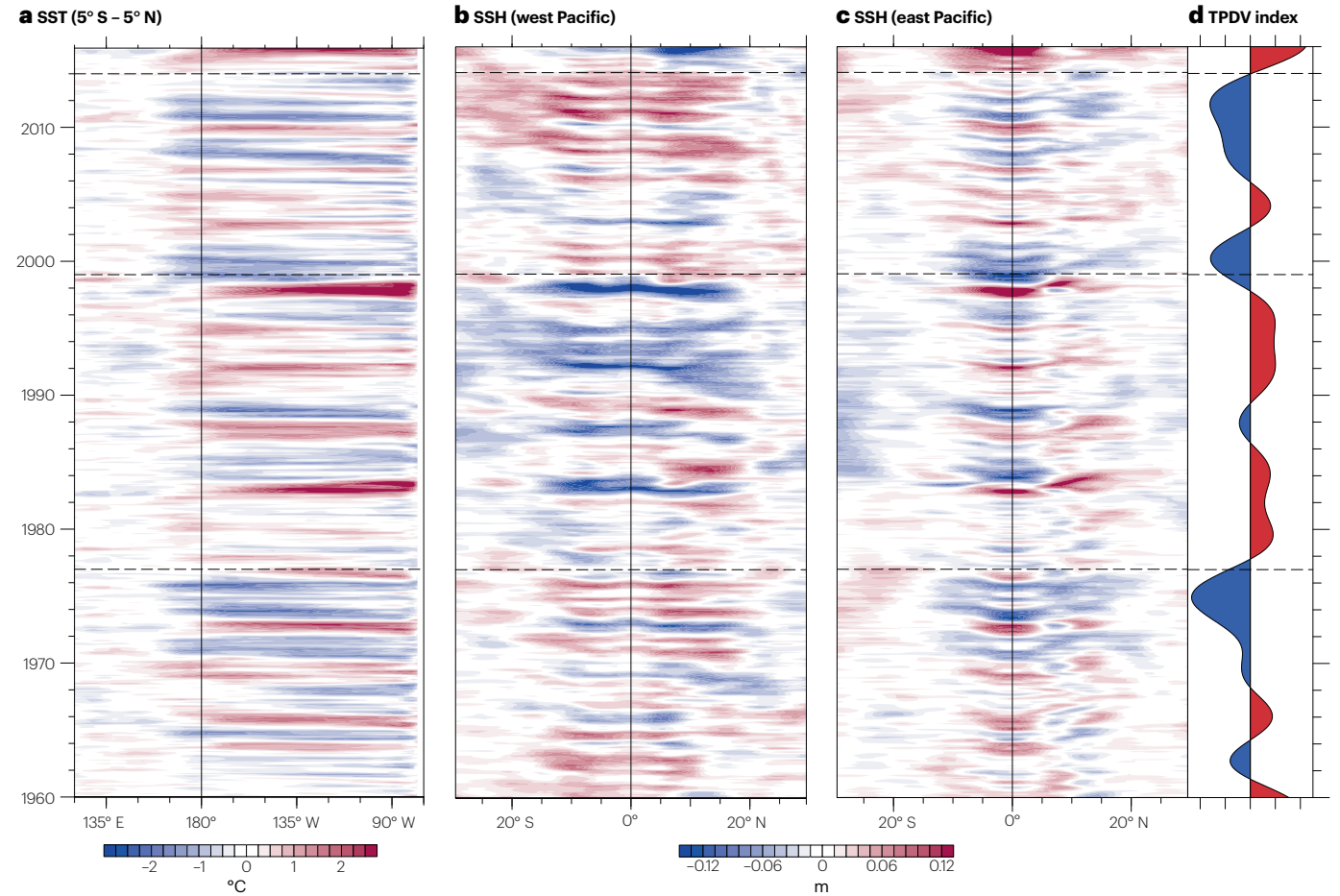

Fig. 2 | Relationship between tropical Pacific decadal variability and El Niño/Southern Oscillation. a, Evolution of sea surface temperature (SST) anomalies[161] averaged over 5° S–5° N, displayed as a function of longitude and time. **b**, Evolution of sea surface height (SSH) anomalies[164], a proxy for upper ocean heat content, averaged west of the dateline, displayed as a function of latitude and time. **c**, As in panel **b**, but SSH anomalies averaged east of the dateline. Anomalies of SST and SSH are obtained by removing the climatological monthly mean and linearly detrending the data over 1958–2015. **d**, Time evolution of the tropical Pacific decadal variability (TPDV) index, computed as the leading principal component of decadal (7–70 years) SST anomalies[161] over 25° S–25° N. More El Niño activity and prevailing negative heat content anomalies in the western tropical Pacific are associated with positive TPDV phases and vice versa.

planetary waves originating in the eastern midlatitudes of both hemispheres with longer transit times in the decadal range[66]. Finally, the timescale of the ocean response to anomalous winds can be extended to the decadal range by the slow eastward propagation of equatorial signals owing to the coupling of oceanic waves with local winds[67]. More generally, decadal timescales cannot be expected to coincide with the transit time of one single wave, but result from the collective effect of multiple waves generated over relatively broad latitude bands at different times, leading to a longer adjustment timescale.

Both mechanisms (advection and planetary wave activity) are likely to contribute to the equatorward propagation of temperature anomalies, with the impact of the South Pacific seemingly dominating spiciness propagation[67–69] owing to its larger and more direct equatorward transport[70–73]. In the North Pacific, the presence of the Intertropical Convergence Zone alters the depth of the pycnocline and creates a potential vorticity barrier[73] that limits the interior equatorward flow[61,73] (Fig. 3a). Global Climate Model sensitivity experiments, in which oceanic temperature and salinity anomalies are blocked from reaching the equator in both hemispheres, indicate that the southern $\bar{v}T'$ process acts as a delayed negative feedback for bi-decadal (12–25 years) variability, whereas oceanic wave adjustment has a dominant influence in the decadal range (9–12 years)[69]. The role of decadal anomalies from the South Pacific is also illustrated by their influence on the evolution of El Niño events during the first decade of the 2000 (ref. 74); cold anomalies in the southwestern tropical Pacific related to the negative TPDV phase during 1999–2014 might have impacted the development of El Niño events[74], possibly leading to the unexpected termination of El Niño in 2014 (ref. 75). Rossby wave activity is also prominent in the North Pacific and provides an important contribution to decadal variability of the equatorial Pacific thermocline[65,66] through the western boundary pathway.

The $v'\overline{T}$ hypothesis

In addition to upwelling of anomalous temperatures from the pycnocline, anomalous upwelling can also drive TPDV via changes in the transport of the STCs (Fig. 3b). Specifically, an increase in the equatorward mass transport of the STCs enhances equatorial upwelling, bringing colder pycnocline waters closer to the surface and cooling SSTs; reduced STC transport has the opposite effect[20]. At interannual timescales, these changes encapsulate the recharge–discharge of the equatorial upper-ocean heat content, underpinning ENSO evolution[76]. The relationship at decadal timescales suggests that similar underlying dynamics might be important at lower frequencies[77].

This hypothesis has been tested in simple models[20,78–80], observations[25,81], ocean general circulation models[82–85] and ocean reanalyses[26,86]. For example, using binned observations of interior transport (zonally averaged pycnocline flow east of the LLWBCs at 9° N and 9° S) as a proxy for STC strength[25] reveals a decline in equatorward subsurface mass convergence after the mid-1970s, concurrent with the tropical Pacific warming associated with the 1976–1977 climate shift[2,25] (Fig. 4a,b). Ocean reanalyses and ocean models forced by observationally constrained surface fields confirm that increased interior equatorward mass convergence is associated with colder equatorial SSTs and vice versa, with high correlations at both interannual and decadal timescales[26,82,86] (Fig. 4c,d). Many climate models also show correlations between transport convergence and SST anomalies that are comparable with those obtained from ocean reanalyses, although some exhibit much weaker relationships[87,88] (Fig. 4e). In addition, transport variability is generally weaker in the models than in observations for the same SST variability[87,88] (Fig. 4f), suggesting a higher sensitivity of modelled SSTs to STC variability.

Besides the interior pycnocline transport, variability of the LLWBCs and ITF can also affect the equatorial mass convergence and equatorial upwelling. Anomalies in the LLWBC transport are of opposite sign to the interior transport anomalies[82,89–91], potentially leading to a partial compensation of interior mass convergence. However, given the complexity of the LLWBCs, and the sparsity of in situ observations in these regions, it is unclear what fraction of their anomalous transport recirculates in the western Pacific, exits the Pacific through the ITF or acts to alter the equatorial mass balance. The strength of the ITF has been shown to contribute to the mass and heat balance of the equatorial Pacific[92] at interannual timescales[93,94], and it could likely influence the equatorial Pacific also at decadal timescales, suggesting a potential oceanic pathway for the Indian Ocean influence on TPDV.

The location of winds that are most influential on STC decadal variations is key to understanding their role in TPDV. Wind variations in subtropical regions could control STC transport and remotely affect equatorial SSTs[20,80]. However, meridional transport changes at each latitude appear to be established by westward-propagating oceanic Rossby waves, as part of the tropical adjustment to varying winds, and be largely controlled by the local wind forcing[26], although influences from the 12°–20° latitude band might also have a role at decadal timescales[22,85,95,96]. The possible origin and nature of these winds are discussed next.

Influences from Pacific extratropical atmospheric forcing

Potential drivers of TPDV are not restricted to the equatorial region. The North Pacific Meridional Mode and South Pacific Meridional Mode[97,98] (NPMM and SPMM, respectively) (Fig. 5a,b) are important in this regard, reflecting SST patterns produced via off-equatorial turbulent heat fluxes and maintained through the wind–evaporation–SST feedback[99]. These modes are important factors influencing equatorial dynamics (for example, through excitation of deep convection near the Intertropical Convergence Zone and corresponding equatorial wind anomalies[100], and heat recharge–discharge in the equatorial pycnocline through meridional flows induced by wind stress curl anomalies — tropical wind charging[101–103]) and thereby ENSO development[97,100,104–106].

However, the NPMM and SPMM are also involved in the development of TPDV. For instance, 'Atm-Slab' models (atmospheric models coupled to slab ocean models)[107,108] exhibit a frequency spectrum reddening of weather and climate variability at decadal timescales through a sequence of extratropical-to-tropical influences (ENSO precursors to ENSO development) and tropical-to-extratropical feedbacks (ENSO teleconnections)[107], as supported by observations[109]. Indeed, model experiments[110] indicate that ENSO teleconnections from the central equatorial Pacific reinforce the NPMM and increase its persistence, resulting in the decadal NPMM variations detected in century-long coral time series from the northeastern subtropical Pacific[111]. Additionally, tropical wind anomalies associated with the Meridional Modes may induce meridional pycnocline flow (as with the Tropical Wind Charging mechanism), providing the atmospheric forcing needed to alter the strength of the STCs and produce equatorial SST anomalies. Sensitivity experiments with simple dynamic models also indicate that extratropical stochastic wind forcing produces low-frequency changes in the equatorial thermocline and multiyear ENSO variations[112].

The impact of the SPMM and NPMM on TPDV is not equal. The influence of the SPMM is thought to dominate[108,113–116]. For instance, idealized nudging of oceanic variability to climatological values over 30° S–10° S caused a ~30% reduction in decadal-scale SST variability in the equatorial Pacific[114]. However, new evidence is emerging for a mode of variability that links the North Pacific with the Central Equatorial Pacific via the NPMM (and thus termed NP–CP mode) at decadal timescales[45,117–119]. This mode involves SST anomalies typical of the NPMM and includes an SSH component with a pattern similar to that typical of decadal differences[118] (Fig. 1c), implying an important role for ocean dynamical processes in TPDV. Thus, both hemispheres can potentially provide the atmospheric forcing for TPDV, but the question of which hemisphere dominates remains outstanding.

Winds of tropical origin

As for extratropical forcing, wind responses to tropical decadal SST anomalies might also be important in driving TPDV. Specifically, SST anomalies in the central equatorial Pacific, where decadal anomalies are more prominent, excite atmospheric Rossby waves, whose subtropical component weakens the subtropical trade winds in both hemispheres[110,120] (Fig. 5a,b). These equatorially forced subtropical wind anomalies then reinforce the equatorial anomaly through thermodynamic (for example, triggering deep convection)[100] or dynamic (for example, through changes in equatorward mass transport induced by the anomalous winds)[26] processes. Accordingly, a feedback loop between equatorial and off-equatorial regions is created, reddening the power spectra and contributing to the meridionally broader SST anomaly pattern found at decadal timescales[18,27].

Low-frequency equatorial SST anomalies also alter the Walker and Hadley circulations, influencing TPDV. In particular, warming along the Pacific equator, mimicking climate change conditions, intensifies the ascending branch of the Hadley circulation, in turn, enhancing off-equatorial trade winds[121–123]. The resulting ocean circulation adjustment leads to strengthened STCs and cooling of the equatorial Pacific at a later time[121] — a delayed negative feedback to the original equatorial

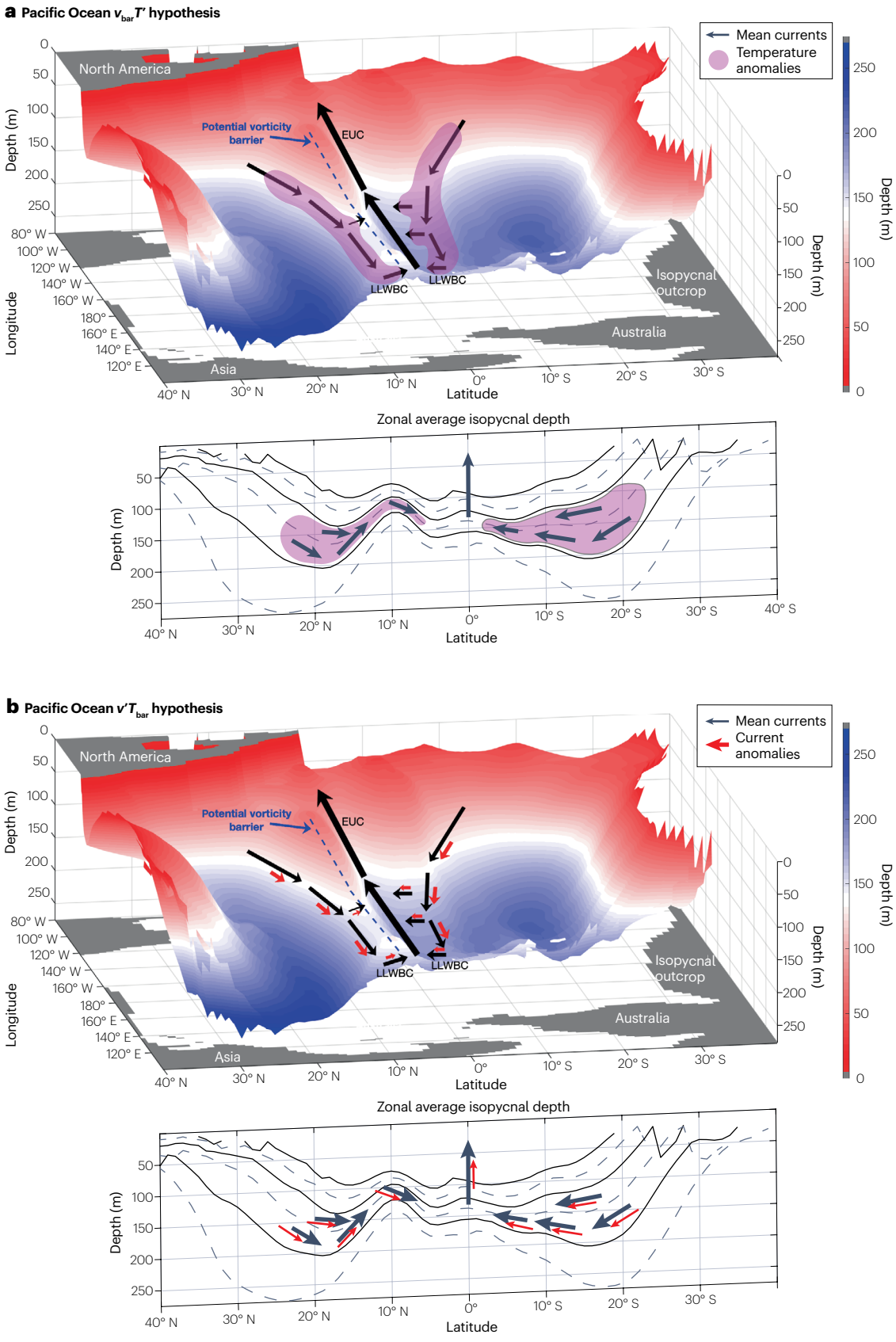
a Pacific Ocean $v_{bar}T'$ hypothesis
Mean currents
Temperature anomalies
North America
Potential vorticity barrier
EUC
LLWBC
LLWBC
Isopycnal outcrop
Australia
Asia
Depth (m)
Longitude
Latitude
Zonal average isopycnal depth
b Pacific Ocean $v'T_{bar}$ hypothesis
Mean currents
Current anomalies
North America
Potential vorticity barrier
EUC
LLWBC
LLWBC
Isopycnal outcrop
Australia
Asia
Depth (m)
Longitude
Latitude
Zonal average isopycnal depth

Fig. 3 | Subtropical cells influence on tropical Pacific decadal variability. **a**, The (compensated) $\bar{v}T'$ mechanism, schematically illustrated in the upper panel as the advection of spiciness anomalies (pink shading) by the mean circulation (black arrows) on the 25.0-kg m^{-3} isopycnal surface. Shading indicates isopycnal depth[163], and the dashed blue line indicates a density ridge in the 5°–10° N latitude band known as the 'potential vorticity barrier'[73]. The lower panel depicts zonally averaged isopycnal depths (from 23 kg m^{-3} to 25.5 kg m^{-3} with a spacing of 0.5 kg m^{-3}; solid lines: 23, 24 and 25 kg m^{-3}; dashed lines: 23.5, 24.5 and 25.5 kg m^{-3}), and the flow of equatorward spiciness anomalies along isopycnal surfaces. **b**, As in panel **a**, but for the $v'\bar{T}$ mechanism, schematically illustrated with mean (black arrows) and anomalous (red arrows) flows, which reveal how flow along isopycnal surfaces connects the subtropics to the tropics. Both $\bar{v}T'$ and $v'\bar{T}$ mechanisms are proposed as potential contributors to tropical Pacific decadal variability. EUC, equatorial undercurrent; LLWBC, low-latitude western boundary current.

SST anomalies[22,123]. Cold decadal conditions in the tropical Pacific have the opposite effect: a weaker Hadley cell, weaker trade winds, weaker STCs and a warmer equatorial Pacific. This feedback loop between equatorial SST anomalies and off-equatorial wind variations supports the view of TPDV as a tropical–extratropical-coupled cyclic mode of variability. However, the ability to robustly detect these links in the relatively short and noisy observational record challenges interpretation.

Influences from other ocean basins

Besides the aforementioned TPDV mechanisms internal to the Pacific, decadal SST variability in the Indian and Atlantic Oceans also has the potential to generate variability in the Pacific[124] via atmospheric teleconnections. These teleconnections occur through a series of atmospheric and oceanic responses to the initial SST, reflecting a Gill-type response[125], as supported by idealized numerical model experiments[37,126–130] (Fig. 5c,d); anomalous atmospheric convection and diabatic heating overlying the initial SST; near-surface zonal wind convergence into the convective region and zonal wind divergence aloft; an eastward-propagating equatorial Kelvin wave emanating away from this heat source and westward-propagating Rossby waves to the north and south of the heat source; and descending motion throughout the rest of the tropics. Alternate Atlantic to Pacific pathways have also been proposed to occur via the midlatitudes along a curved pathway through the North Pacific to the western equatorial Pacific[131,132] or through the tropics owing to SLP difference and induced surface wind changes across the Panama Isthmus[133–135]. Similarly, the linkages between the Indian and Pacific Ocean can occur via wind changes across the Maritime Continent[37] or through stationary extratropical wave trains[136].

Collectively, these changes influence TPDV. They alter the global Walker circulation on intraseasonal through multidecadal timescales[23,24,126,128,137–140], spreading the diabatically generated tropospheric temperature anomaly through the entire tropics (the weak temperature gradient approximation)[141,142] and increasing the vertical stability of the troposphere (the tropospheric temperature mechanism)[143]. All three of these processes can alter the Pacific trade winds leading to changes in central-eastern Pacific SSTs that can be further amplified owing to the tightly coupled nature of the atmosphere–ocean system in the tropical Pacific[128,137,144].

Through these mechanisms, observations suggest that TPDV has responded to Atlantic and Indian Ocean SST forcing. For instance, Atlantic warming had a prominent role in the transition from a positive TPDV in the 1990s to a negative TPDV in the early 2000s[11,23,128,130,139]. This importance can be linked to the fact that the Atlantic-Rossby wave-induced wind anomalies modulate winds in the tropical Pacific, and this surface wind modulation is strongest in the central Pacific where the Rossby and Kelvin waves collide (Fig. 5c,d). This strong effect of the Atlantic on the Pacific is likely to have been relatively consistent from 1870 onwards, although its dominance might have been different in the past[124,131,145]. By contrast, the influence of the Indian Ocean in isolation is thought to be minor during the TPDV transition in the early 2000s[23,126] or more important in amplifying the Pacific response to Atlantic forcing[128]. Yet, the magnitude of the Pacific response to idealized Indian Ocean SST forcing is more prominent over longer periods, as during 1980–2010 and 1958–2010 (refs. 24,136).

However, there are limitations in understanding the influence of other ocean basins in driving TPDV. Uncertainties arise from discrepancies between some model results. For example, although inter-basin interactions are thought to amplify TPDV, model simulations in which the Atlantic or Indian Ocean influence is removed instead suggest that TPDV is intensified in the absence of Atlantic or Indian Ocean coupling[146,147]. Also, the connection between the Atlantic and Pacific becomes less clear when partially coupled numerical experiments become more realistic[148]. These uncertainties indicate possible limitations of currently used partially coupled experiments[149].

Summary and future perspectives

TPDV of 7–70 years is linked to coherent basin-scale SST and SLP anomalies, with global impacts. Despite a limited historical record of subsurface data, surface manifestations of TPDV are also associated with a reorganization of tropical Pacific upper-ocean heat content, most notably in the zonal direction, suggesting the involvement of ocean dynamical processes. Indeed, several mechanisms have been proposed to explain TPDV. Although it is plausible it might simply arise as a residual of random ENSO variations[18,38], TPDV leads decadal ENSO modulation by a few years[51]. This lead–lag relationship suggests that ENSO decadal changes are likely a consequence of the slowly varying background conditions, not their cause. A strong relationship between decadal variations in the strength of the STCs and equatorial SSTAs provides support for the $v'\bar{T}$ hypothesis. However, the largest correlations occur at zero lag, making a causal relationship between STC transport and equatorial SST changes unlikely. Instead, concurrent STC and equatorial SST variations are part of the tropical pycnocline adjustment to varying wind forcing, mediated by Rossby wave activity[26].

Thus, these wave-mediated adjustment processes, encompassing the non-compensated component of the $\bar{v}T'$ hypothesis, emerge as a robust feature of TPDV. For instance, Rossby wave activity alters pycnocline depth and manifests itself as temperature anomalies that propagate on mean isopycnals, contributing to TPDV given their transit times and interaction with the forcing, the latter including preferential response to the larger spatial and temporal scales of the winds[65]. Propagation of salinity-compensated temperature anomalies (spiciness anomalies) is also supported in modelling contexts as a potential mechanism[61,63]. Yet, limited observational evidence of anomalies reaching the equatorial region, in addition to a small modelled influence[59], call into question the magnitude of the compensated $\bar{v}T'$ component. The atmospheric response to decadal SSTAs in the equatorial Pacific, internal atmospheric variability in the extratropical Pacific and atmospheric influences from the Atlantic and Indian Oceans are all potentially important drivers of the aforementioned oceanic processes.

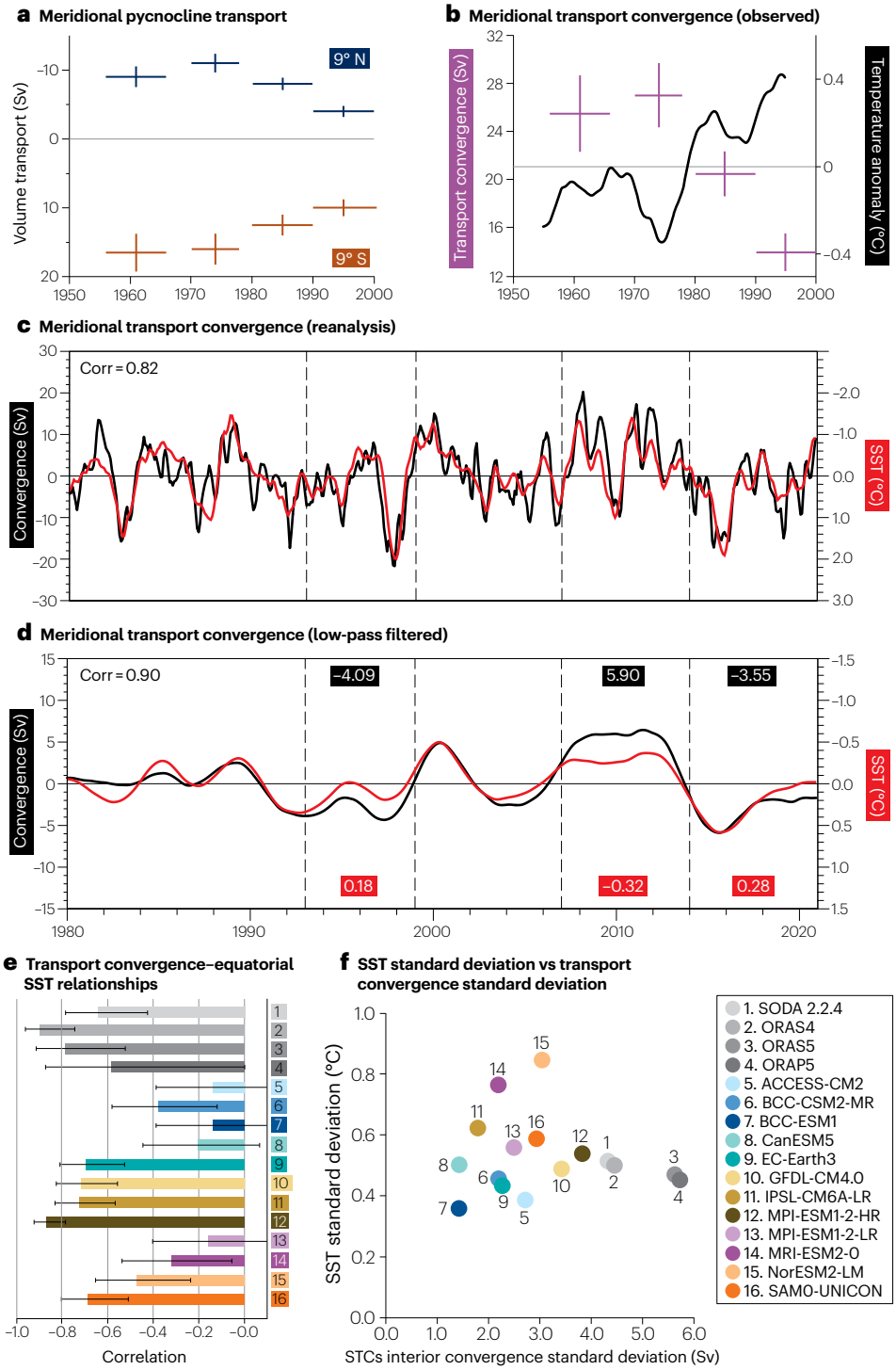

Fig. 4 | Assessment of the $v'\overline{T}$ hypothesis. **a**, Observed mean zonally integrated interior meridional pycnocline transports at 9° N and 9° S, computed over 1956–1965, 1970–1977, 1980–1989 and 1990–1999. **b**, Observed mean meridional transport convergence across 9° N and 9° S (purple), computed as the difference between Southern and Northern Hemisphere transports, and sea surface temperature (SST) anomalies averaged over the central and eastern equatorial Pacific (black line; 9° N–9° S, 90° W–180° W). Error bars represent one standard error. **c**, Reanalysis interior meridional transport convergence anomalies[165] (seasonal cycle removed) across 9.5° N and 9.5° S in the Pacific (black), and SST anomalies averaged over 9.5° N–9.5°S, 90° W–180° W (red). Meridional velocity anomalies used to compute transports, and SST anomalies are linearly detrended. The value in the top left indicates correlation at zero lag between the time series. **d**, Same as panel **c** but for 7-year low-pass-filtered anomalies. Values indicate mean decadal transport convergence and SST anomalies between vertical dashed lines. **e**, Correlations between transport convergence at 9° N and 9° S and equatorial SST anomalies in 4 ocean reanalyses[163,164,166,167] and 12 CMIP6 historical simulations. Error bars represent the 95% confidence interval. **f**, Standard deviation of equatorial SST anomalies versus the standard deviation of transport convergence at 9° N and 9° S for the same ocean reanalyses and historical CMIP6 simulations in panel **e**. Zonally averaged pycnocline transport convergence and equatorial SST anomalies are highly correlated in observations, ocean reanalyses and several climate models. STC, subtropical cell. Panels **a** and **b** reprinted from ref. 25, Springer Nature Limited. Panels **c** and **d** reprinted with permission from ref. 26, AMS. Panels **e** and **f** reprinted from ref. 88, Springer Nature Limited.

However, it is clear that many questions still remain about the nature of TPDV. There are some similarities between TPDV and ENSO, but while ENSO is an ocean–atmosphere coupled phenomenon, whose growth and phase transitions rely on coupled feedbacks, it is not clear whether the same is true for TPDV. Although there are indications that low-frequency equatorial heating[121] or individual ENSO events[43] induce off-equatorial winds favourable for a TPDV phase reversal, there is still uncertainty about the origin and nature of the winds involved. Internally generated wind anomalies in the subtropical-tropical regions create equatorial SST anomalies[21], which then reinforce the subtropical wind anomalies through atmospheric teleconnections, increasing their persistence to enhance

lower-frequency variability[110]. Decadal timescale SST anomalies in the Atlantic and Indian Oceans also induce wind anomalies in the tropical Pacific conducive to the development of SST anomalies of the opposite sign[23,127,128,130]. However, the extent to which wind forcing from the extratropics or from other ocean basins might itself be the result of forcing from the tropical Pacific is not clearly understood. Furthermore, the relative magnitude of these various sources of wind variability in forcing TPDV is not known. A further uncertainty is related to whether the wind variations arise from deterministic processes operating on decadal timescales, or whether the decadal timescale processes in the Pacific are simply the result of stochastic white noise forcing that the ocean integrates through its inertia to produce a red noise spectral response. A full understanding of TPDV requires all these outstanding uncertainties be resolved.

Properly designed coupled model sensitivity experiments, in which SSTs are prescribed in certain regions, could be used to isolate the contribution of the different regional sources of wind anomalies. As these experiments can be affected by model biases and might be difficult to interpret[149], they should be complemented by analyses of multivariate empirical models[150], which are trained on observations and allow a cleaner decoupling of feedbacks among different variables and regions[151–153]. In addition, simple ocean models that capture Rossby wave dynamics[26,154] can help to assess the role of different aspects of the winds, including location and spectral characteristics, in reproducing key features of TPDV.

Although spiciness anomalies do not seem to substantially affect TPDV, current evidence is based on a limited number of analyses using just over two decades of observations from Argo floats and primarily conducted with ocean-only models. However, the expected

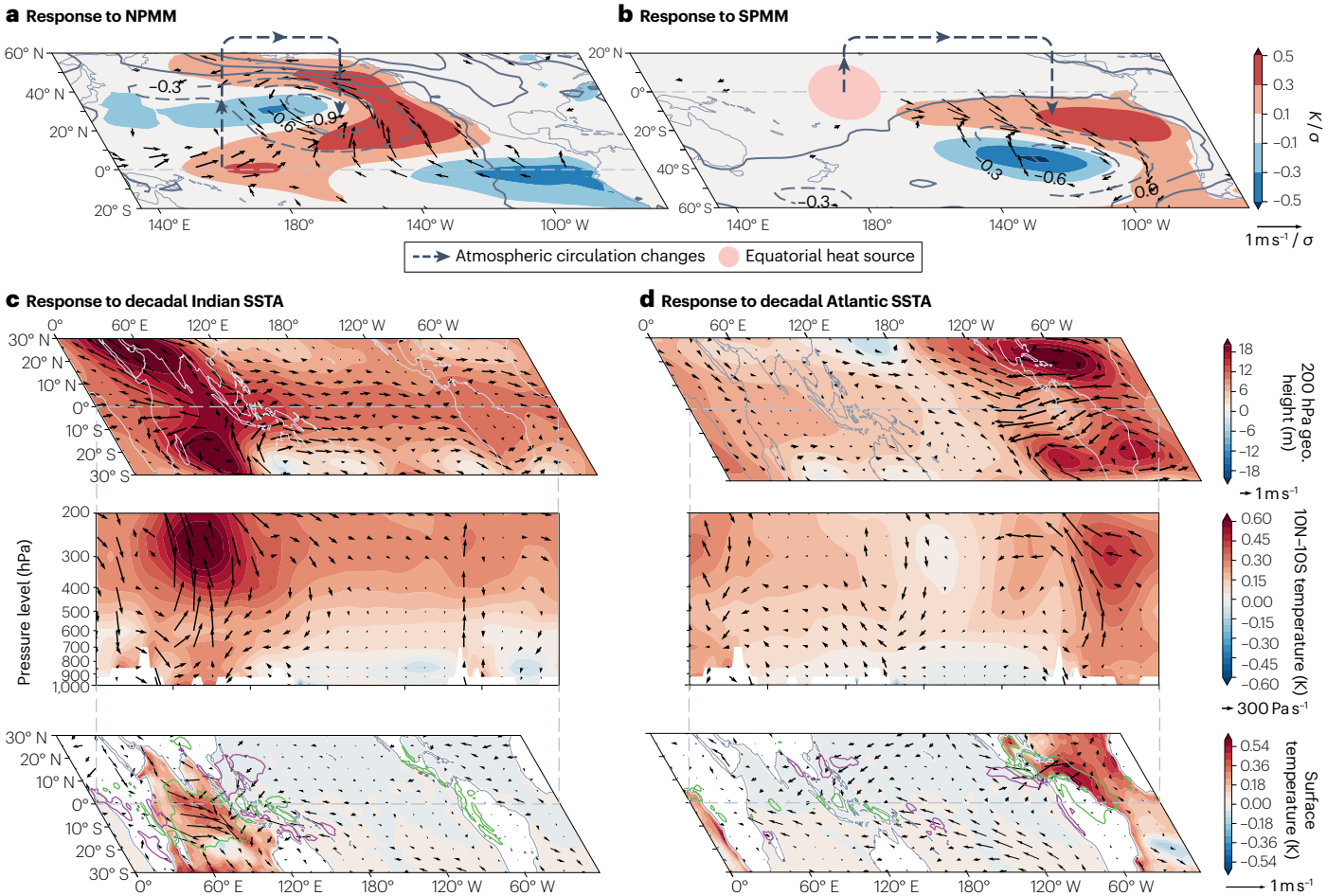

Fig. 5 | Atmospheric processes involved in tropical Pacific decadal variability. a, Regressions of sea surface temperature (SST; shading)[161], sea-level pressure (contours)[162] and surface wind[162] anomalies on the North Pacific Meridional Mode (NPMM) index; the NPMM index is calculated as the first SST expansion time series of an SST-wind maximum covariance analysis (with Niño3.4 index influence removed) performed over 21° S–32° N, 175° E–95° W (ref. 98). **b**, As in panel **a**, but for the South Pacific Meridional Mode (SPMM); the SPMM index is calculated as the NPMM, but over 10° S–35° S, 180° E–70° W (ref. 168). **c**, Modelled multidecadal average atmospheric response to decadal Indian Ocean SST anomalies[169] (bottom, shading; representing SST differences from 1999–2008 minus 1988–1998), including precipitation (bottom, contours; green indicates positive anomalies and purple indicates negative anomalies), surface winds (bottom, vectors), 10° S–10° N mean temperature (middle, shading) and vertical winds (middle, vectors; magnified by a factor of 300 to scale with the zonal wind), and 200 hPa geopotential height (top, shading) and winds (top, vectors). **d**, As in panel **c**, but the response to decadal Atlantic Ocean SST anomalies (1999–2014 minus 1982–1998)[145]. Atmospheric influences from the extratropical Pacific, Atlantic and Indian Oceans can modify Pacific equatorial winds and contribute to tropical Pacific decadal variability. SSTA, sea surface temperature anomaly.

Box 2

Paleoclimate insights

The brevity of the instrumental record limits analyses of tropical Pacific decadal variability (TPDV) with instrumental observations. Paleoclimate proxies, particularly tropical corals and sclerosponges, provide opportunities to track the low-frequency variations of the tropical oceans over centuries. Over the most recent phase transitions of TPDV, corals have recorded associated changes in dynamically relevant fields, including sea surface temperature[171,172], salinity[173–175], westerly wind bursts[176] and upwelling[177,178]. Proxy records have provided evidence of interactions among different ocean basins at both interannual[179] and decadal[180] timescales. Proxy records from the Eastern Subtropical North Pacific, where sea surface temperature anomalies might reflect NPMM activity, illustrate high levels of decadal variability coherent with the Central Equatorial Pacific records, supporting the potential involvement of the NPMM in TPDV[174].

Additionally, paleoclimate analyses provide a perspective into the range of TPDV found over centuries-millennia, which can be used to assess model simulations of TPDV. The figure compares TPDV across five different instrumental products[161,181–184], two generations of climate models (CMIP5, CMIP6, historical[185,186] and Past1000 (refs. 187,188) experiments) and three different sources of paleo data (coral $\delta^{18}O$ from the central and eastern equatorial Pacific[189–191], field reconstructions[192,193] and paleo data assimilation products[194,195]) using violin plots[196]. The number of data sets used for each violin is indicated by *N*. TPDV is described in terms of the standard deviation of decadal variations (7–70 years) of the Niño3.4 index (annually averaged sea surface temperature anomalies in the 5° S–5° N, 170° W–120° W region).

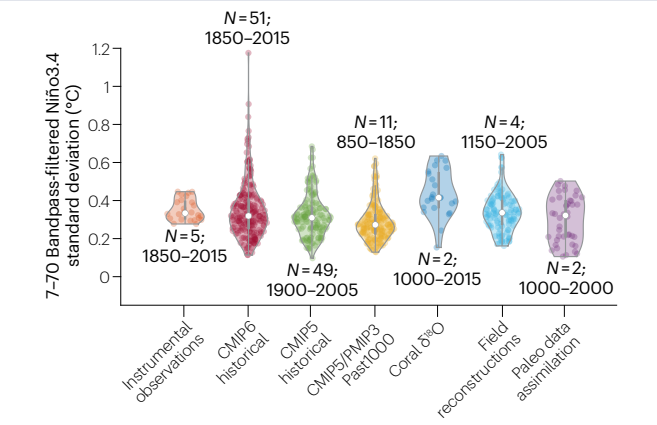

Violin plots for each data set are based on decadal standard deviations of 100-year sliding windows allowing for 50 years overlap between segments. Individual dots represent the decadal standard deviation of each unique 100-year segment. The median and interquartile range of these values is indicated by the white dots and vertical lines, respectively, whereas the width of the violin plot for each standard deviation indicates the corresponding frequency of occurrence. Notably, the instrumental record does not cover the full range of decadal variability suggested by both paleoclimate proxy reconstructions and climate models, although the median standard deviation is very similar among products.

concentration of variance at decadal timescales of spiciness anomalies arriving at the equator, and the resulting rearrangement of the tropical climate, suggests that spiciness anomalies could still be a potentially important driver of TPDV in the coupled setting. Thus, the role of spiciness should be further investigated in the context of coupled models. Availability of long time series from model simulations with realistic mixing parameterizations, achieved through either higher spatial resolution or improved model design, would be critical to more reliably assess the impact of spiciness on TPDV.

Finally, a major limitation in our understanding of TPDV stems from the relatively short observational record, which does not allow a robust characterization of decadal variability, and a proper assessment of climate models fidelity in simulating it. More extensive investigations of TPDV using multicentury paleoclimate records could provide critical insights on the key features of TPDV and better constrain climate models evaluation at decadal timescales (Box 2).

This Review has not addressed the question of how TPDV might change in response to external forcing. However, changes in the characteristics of TPDV as a result of anthropogenic forcing can be expected. Increasing surface temperatures will result in increased ocean stratification[155], leading to faster Rossby wave propagation, shorter adjustment timescales and reduced growth and predictability of Pacific decadal variability[156], which might lead to weaker, shorter timescale TPDV in the future[157]. The expected reduced influence of Atlantic variability on ENSO owing to increased tropospheric stability[158] can also reduce the influence of Atlantic decadal variability on TPDV. Yet, the wind–evaporation–SST feedback is projected to increase owing to warmer sea surface temperatures and increased evaporative response, leading to an enhanced impact of the NPMM on ENSO and possibly on TPDV[159,160]. These, and other possible processes and their interactions, need to be assessed in climate models to determine how TPDV might change in a warmer world.

Published online: 18 October 2023

References

1. Lyu, K., Zhang, X., Church, J. A., Hu, J. & Yu, J.-Y. Distinguishing the quasi-decadal and multidecadal sea level and climate variations in the Pacific: implications for the ENSO-like low-frequency variability. *J. Clim.* **30**, 5097–5117 (2017).
2. Mantua, N. J., Hare, S. R., Zhang, Y., Wallace, J. M. & Francis, R. C. A Pacific interdecadal climate oscillation with impacts on salmon production. *Bull. Am. Meteorol. Soc.* **78**, 1069–1080 (1997).
3. Henley, B. J. et al. A tripole index for the interdecadal Pacific oscillation. *Clim. Dyn.* **45**, 3077–3090 (2015).
4. Okumura, Y. M., Sun, T. & Wu, X. Asymmetric modulation of El Niño and La Niña and the linkage to tropical Pacific decadal variability. *J. Clim.* **30**, 4705–4733 (2017).
5. Capotondi, A., Deser, C., Phillips, A. S., Okumura, Y. & Larson, S. M. ENSO and Pacific decadal variability in the community earth system model version 2. *J. Adv. Model. Earth Syst.* **12**, e2019MS002022 (2020).
6. Li, X. et al. Tropical teleconnection impacts on Antarctic climate changes. *Nat. Rev. Earth Environ.* **2**, 680–698 (2021).
7. Heidemann, H. et al. Variability and long-term change in Australian monsoon rainfall: a review. *WIREs Clim. Change* **14**, e823 (2023).

8. Maher, N., Kay, J. E. & Capotondi, A. Modulation of ENSO teleconnections over North America by the Pacific decadal oscillation. *Environ. Res. Lett.* **17**, 114005 (2022).
9. Kosaka, Y. & Xie, S.-P. Recent global-warming hiatus tied to equatorial Pacific surface cooling. *Nature* **501**, 403–407 (2013).
10. Meehl, G. A., Hu, A., Santer, B. D. & Xie, S.-P. Contribution of the interdecadal Pacific oscillation to twentieth-century global surface temperature trends. *Nat. Clim. Change* **6**, 1005–1008 (2016).
11. England, M. H. et al. Recent intensification of wind-driven circulation in the Pacific and the ongoing warming hiatus. *Nat. Clim. Change* **4**, 222–227 (2014).
12. Kociuba, G. & Power, S. B. Inability of CMIP5 models to simulate recent strengthening of the walker circulation: implications for projections. *J. Clim.* **28**, 20–35 (2015).
13. McGregor, S., Stuecker, M. F., Kajtar, J. B., England, M. H. & Collins, M. Model tropical Atlantic biases underpin diminished Pacific decadal variability. *Nat. Clim. Change* **8**, 493–498 (2018).
14. Weller, E. et al. Human-caused Indo-Pacific warm pool expansion. *Sci. Adv.* **2**, e1501719 (2016).
15. Hu, S. et al. Deep-reaching acceleration of global mean ocean circulation over the past two decades. *Sci. Adv.* **6**, eaax7727 (2020).
16. Ummenhofer, C. C., Murty, S. A., Sprintall, J., Lee, T. & Abram, N. J. Heat and freshwater changes in the Indian Ocean region. *Nat. Rev. Earth Environ.* **2**, 525–541 (2021).
17. Luo, J.-J., Wang, G. & Dommenget, D. May common model biases reduce CMIP5's ability to simulate the recent Pacific La Niña-like cooling? *Clim. Dyn.* **50**, 1335–1351 (2018).
18. Power, S. et al. Decadal climate variability in the tropical Pacific: characteristics, causes, predictability, and prospects. *Science* **374**, eaay9165 (2021).
19. Gu, D. & Philander, S. Interdecadal climate fluctuations that depend on exchanges between the tropics and extratropics. *Science* **275**, 805–807 (1997).
20. McCreary, J. P. & Lu, P. Interaction between the subtropical and equatorial ocean circulations: the subtropical cell. *J. Phys. Oceanogr.* **24**, 466–497 (1994).
21. Vimont, D. J., Battisti, D. S. & Hirst, A. C. Footprinting: a seasonal connection between the tropics and mid-latitudes. *Geophys. Res. Lett.* **28**, 3923–3926 (2001).
22. Meehl, G. A. & Hu, A. Megadroughts in the Indian monsoon region and Southwest North America and a mechanism for associated multidecadal Pacific sea surface temperature anomalies. *J. Clim.* **19**, 1605–1623 (2006).
23. McGregor, S. et al. Recent walker circulation strengthening and Pacific cooling amplified by Atlantic warming. *Nat. Clim. Change* **4**, 888–892 (2014).
24. Luo, J.-J., Sasaki, W. & Masumoto, Y. Indian Ocean warming modulates Pacific climate change. *Proc. Natl Acad. Sci. USA* **109**, 18701–18706 (2012).
25. McPhaden, M. J. & Zhang, D. Slowdown of the meridional overturning circulation in the upper Pacific Ocean. *Nature* **415**, 603–608 (2002).
26. Capotondi, A. & Qiu, B. Decadal variability of the Pacific shallow overturning circulation and the role of local wind forcing. *J. Clim.* **36**, 1001–1015 (2023).
27. Zhang, Y., Wallace, J. M. & Battisti, D. S. ENSO-like interdecadal variability: 1900–93. *J. Clim.* **10**, 1004–1020 (1997).
28. Qiu, B. & Chen, S. Multidecadal sea level and gyre circulation variability in the northwestern tropical Pacific Ocean. *J. Phys. Oceanogr.* **42**, 193–206 (2012).
29. Hu, S. et al. Multi-decadal trends in the tropical Pacific western boundary currents retrieved from historical hydrological observations. *Sci. China Earth Sci.* **64**, 600–610 (2021).
30. Maher, N., England, M. H., Gupta, A. S. & Spence, P. Role of Pacific trade winds in driving ocean temperatures during the recent slowdown and projections under a wind trend reversal. *Clim. Dyn.* **51**, 321–336 (2018).
31. Nieves, V., Willis, J. K. & Patzert, W. C. Recent hiatus caused by decadal shift in Indo-Pacific heating. *Science* **349**, 532–535 (2015).
32. Lee, S.-K. et al. Pacific origin of the abrupt increase in Indian Ocean heat content during the warming hiatus. *Nat. Geosci.* **8**, 445–449 (2015).
33. Lee, T. & McPhaden, M. J. Decadal phase change in large-scale sea level and winds in the Indo-Pacific region at the end of the 20th century. *Geophys. Res. Lett.* **35**, L01605 (2008).
34. Li, Y., Han, W., Hu, A., Meehl, G. A. & Wang, F. Multidecadal changes of the upper Indian Ocean heat content during 1965–2016. *J. Clim.* **31**, 7863–7884 (2018).
35. Merrifield, M. A. & Maltrud, M. E. Regional sea level trends due to a Pacific trade wind intensification. *Geophys. Res. Lett.* **38**, L21605 (2011).
36. McGregor, S., Gupta, A. S. & England, M. H. Constraining wind stress products with sea surface height observations and implications for Pacific Ocean sea level trend attribution. *J. Clim.* **25**, 8164–8176 (2012).
37. Han, W. et al. Intensification of decadal and multi-decadal sea level variability in the western tropical Pacific during recent decades. *Clim. Dyn.* **43**, 1357–1379 (2014).
38. Vimont, D. J. The contribution of the interannual ENSO cycle to the spatial pattern of decadal ENSO-like variability. *J. Clim.* **18**, 2080–2092 (2005).
39. Capotondi, A., Wittenberg, A. T., Kug, J.-S., Takahashi, K. & McPhaden, M. J. *El Niño Southern Oscillation in a Changing Climate* (eds McPhaden, M. J., Santoso, A. & Cai, W.) 65–86 (AGU, 2020).
40. McPhaden, M. J., Lee, T. & McClurg, D. El Niño and its relationship to changing background conditions in the tropical Pacific Ocean. *Geophys. Res. Lett.* **38**, L15709 (2011).
41. McPhaden, M. J. Genesis and evolution of the 1997-98 El Nino. *Science* **283**, 950–954 (1999).
42. Capotondi, A., Sardeshmukh, P. D. & Ricciardulli, L. The nature of the stochastic wind forcing of ENSO. *J. Clim.* **31**, 8081–8099 (2018).
43. Meehl, G. A., Teng, H., Capotondi, A. & Hu, A. The role of interannual ENSO events in decadal timescale transitions of the Interdecadal Pacific Oscillation. *Clim. Dyn.* **57**, 1933–1951 (2021).
44. Gordon, E. M., Barnes, E. A. & Hurrell, J. W. Oceanic harbingers of Pacific decadal oscillation predictability in CESM2 detected by neural networks. *Geophys. Res. Lett.* **48**, e2021GL095392 (2021).
45. Liu, C., Zhang, W., Jin, F.-F., Stuecker, M. F. & Geng, L. Equatorial origin of the observed tropical Pacific quasi-decadal variability from ENSO nonlinearity. *Geophys. Res. Lett.* **49**, e2022GL097903 (2022).
46. Capotondi, A. & Sardeshmukh, P. D. Is El Niño really changing? *Geophys. Res. Lett.* **44**, 8548–8556 (2017).
47. Fedorov, A. V. & Philander, S. G. Is El Niño changing? *Science* **288**, 1997–2002 (2000).
48. Zhao, M., Hendon, H. H., Alves, O., Liu, G. & Wang, G. Weakened Eastern Pacific El Niño predictability in the early twenty-first century. *J. Clim.* **29**, 6805–6822 (2016).
49. Wang, G. & Hendon, H. H. Why 2015 was a strong El Niño and 2014 was not. *Geophys. Res. Lett.* **44**, 8567–8575 (2017).
50. Kim, G.-I. & Kug, J.-S. Tropical Pacific decadal variability induced by nonlinear rectification of El Niño–Southern Oscillation. *J. Clim.* **33**, 7289–7302 (2020).
51. Zhang, Y. et al. Role of ocean dynamics in equatorial Pacific decadal variability. *Clim. Dyn.* **59**, 2517–2529 (2022).
52. Zhao, Y., Di Lorenzo, E., Newman, M., Capotondi, A. & Stevenson, S. A Pacific tropical decadal variability challenge for climate models. *Geophys. Res. Lett.* **50**, e2023GL104037 (2023).
53. Munk, W. in *Evolution of Physical Oceanography* (eds Warren, B. A. & Wunsch, C.) 264–291 (MIT Press, 1981).
54. Schneider, N. A decadal spiciness mode in the tropics. *Geophys. Res. Lett.* **27**, 257–260 (2000).
55. Yeager, S. G. & Large, W. G. Late-winter generation of spiciness on subducted isopycnals. *J. Phys. Oceanogr.* **34**, 1528–1547 (2004).
56. Yeager, S. G. & Large, W. G. Observational evidence of winter spice injection. *J. Phys. Oceanogr.* **37**, 2895–2919 (2007).
57. Sasaki, Y. N., Schneider, N., Maximenko, N. & Lebedev, K. Observational evidence for propagation of decadal spiciness anomalies in the North Pacific. *Geophys. Res. Lett.* **37**, L07708 (2010).
58. Kolodziejczyk, N. & Gaillard, F. Observation of spiciness interannual variability in the Pacific pycnocline. *J. Geophys. Res. Oceans* **117**, C12018 (2012).
59. Zeller, M. *The Impact of Subtropical to Tropical Oceanic Interactions on Tropical Pacific Decadal Variability.* Thesis, Monash Univ. (2020).
60. Alberty, M. S. et al. Spatial patterns of mixing in the Solomon Sea. *J. Geophys. Res. Ocean.* **122**, 4021–4039 (2017).
61. Zeller, M., McGregor, S., van Sebille, E., Capotondi, A. & Spence, P. Subtropical–tropical pathways of spiciness anomalies and their impact on equatorial Pacific temperature. *Clim. Dyn.* **56**, 1131–1144 (2021).
62. Kilpatrick, T., Schneider, N. & Di Lorenzo, E. Generation of low-frequency spiciness variability in the thermocline. *J. Phys. Oceanogr.* **41**, 365–377 (2011).
63. Schneider, N. The response of tropical climate to the equatorial emergence of spiciness anomalies. *J. Clim.* **17**, 1083–1095 (2004).
64. Capotondi, A. & Alexander, M. A. Rossby waves in the tropical North Pacific and their role in decadal thermocline variability. *J. Phys. Oceanogr.* **31**, 3496–3515 (2001).
65. Capotondi, A., Alexander, M. A. & Deser, C. Why are there Rossby wave maxima in the Pacific at 10° S and 13° N. *J. Phys. Oceanogr.* **33**, 1549–1563 (2003).
66. Galanti, E. & Tziperman, E. A midlatitude–ENSO teleconnection mechanism via baroclinically unstable long Rossby waves. *J. Phys. Oceanogr.* **33**, 1877–1888 (2003).
67. Luo, J.-J. & Yamagata, T. Long-term El Niño–Southern Oscillation (ENSO)-like variation with special emphasis on the South Pacific. *J. Geophys. Res. Ocean.* **106**, 22211–22227 (2001).
68. Luo, J.-J. et al. South Pacific origin of the decadal ENSO-like variation as simulated by a coupled GCM. *Geophys. Res. Lett.* **30**, 2250 (2003).
69. Tatebe, H., Imada, Y., Mori, M., Kimoto, M. & Hasumi, H. Control of decadal and bidecadal climate variability in the tropical Pacific by the Off-Equatorial South Pacific Ocean. *J. Clim.* **26**, 6524–6534 (2013).
70. Johnson, G. C. & McPhaden, M. J. Interior pycnocline flow from the subtropical to the Equatorial Pacific Ocean. *J. Phys. Oceanogr.* **29**, 3073–3089 (1999).
71. Nonaka, M. & Xie, S.-P. Propagation of North Pacific interdecadal subsurface temperature anomalies in an ocean GCM. *Geophys. Res. Lett.* **27**, 3747–3750 (2000).
72. Zeller, M., McGregor, S. & Spence, P. Hemispheric asymmetry of the Pacific shallow meridional overturning circulation. *J. Geophys. Res. Ocean.* **124**, 5765–5786 (2019).
73. Lu, P. & McCreary, J. P. Influence of the ITCZ on the flow of thermocline water from the subtropical to the Equatorial Pacific Ocean. *J. Phys. Oceanogr.* **25**, 3076–3088 (1995).
74. Imada, Y., Tatebe, H., Watanabe, M., Ishii, M. & Kimoto, M. South Pacific influence on the termination of El Niño in 2014. *Sci. Rep.* **6**, 30341 (2016).
75. McPhaden, M. J. Playing hide and seek with El Niño. *Nat. Clim. Change* **5**, 791–795 (2015).
76. Jin, F.-F. An equatorial ocean recharge paradigm for ENSO. Part I: conceptual model. *J. Atmos. Sci.* **54**, 811–829 (1997).
77. Wang, X., Jin, F.-F. & Wang, Y. A tropical ocean recharge mechanism for climate variability. Part II: a unified theory for decadal and ENSO modes. *J. Clim.* **16**, 3599–3616 (2003).
78. Kleeman, R., McCreary, J. P. Jr. & Klinger, B. A. A mechanism for generating ENSO decadal variability. *Geophys. Res. Lett.* **26**, 1743–1746 (1999).

79. Klinger, B. A., McCreary, J. P. & Kleeman, R. The relationship between oscillating subtropical wind stress and equatorial temperature. *J. Phys. Oceanogr.* **32**, 1507–1521 (2002).
80. Solomon, A., McCreary, J. P., Kleeman, R. & Klinger, B. A. Interannual and decadal variability in an intermediate coupled model of the Pacific region. *J. Clim.* **16**, 383–405 (2003).
81. McPhaden, M. J. & Zhang, D. Pacific Ocean circulation rebounds. *Geophys. Res. Lett.* **31**, L18301 (2004).
82. Capotondi, A., Alexander, M. A., Deser, C. & McPhaden, M. J. Anatomy and decadal evolution of the Pacific subtropical–tropical cells (STCs). *J. Clim.* **18**, 3739–3758 (2005).
83. Cheng, W., McPhaden, M. J., Zhang, D. & Metzger, E. J. Recent changes in the Pacific subtropical cells inferred from an eddy-resolving ocean circulation model. *J. Phys. Oceanogr.* **37**, 1340–1356 (2007).
84. Lübbecke, J. F., Böning, C. W. & Biastoch, A. Variability in the subtropical–tropical cells and its effect on near-surface temperature of the equatorial Pacific: a model study. *Ocean Sci.* **4**, 73–88 (2008).
85. Farneti, R., Dwivedi, S., Kucharski, F., Molteni, F. & Griffies, S. M. On Pacific subtropical cell variability over the second half of the twentieth century. *J. Clim.* **27**, 7102–7112 (2014).
86. Schott, F. A., Stramma, L., Wang, W., Giese, B. S. & Zantopp, R. Pacific subtropical cell variability in the SODA 2.0.2/3 assimilation. *Geophys. Res. Lett.* **35**, L10607 (2008).
87. Zhang, D. & McPhaden, M. J. Decadal variability of the shallow Pacific meridional overturning circulation: relation to tropical sea surface temperatures in observations and climate change models. *Ocean Model.* **15**, 250–273 (2006).
88. Graffino, G., Farneti, R. & Kucharski, F. Low-frequency variability of the Pacific subtropical cells as reproduced by coupled models and ocean reanalyses. *Clim. Dyn.* **56**, 3231–3254 (2021).
89. Lee, T. & Fukumori, I. Interannual-to-decadal variations of tropical–subtropical exchange in the Pacific Ocean: boundary versus interior pycnocline transports. *J. Clim.* **16**, 4022–4042 (2003).
90. Zilberman, N. V., Roemmich, D. H. & Gille, S. T. The mean and the time variability of the shallow meridional overturning circulation in the tropical South Pacific ocean. *J. Clim.* **26**, 4069–4087 (2013).
91. Kessler, W. S., Hristova, H. G. & Davis, R. E. Equatorward western boundary transport from the South Pacific: glider observations, dynamics and consequences. *Prog. Oceanogr.* **175**, 208–225 (2019).
92. Mayer, M., Haimberger, L. & Balmaseda, M. A. On the energy exchange between tropical ocean basins related to ENSO. *J. Clim.* **27**, 6393–6403 (2014).
93. Mayer, M., Alonso Balmaseda, M. & Haimberger, L. Unprecedented 2015/2016 Indo-Pacific heat transfer speeds up tropical Pacific heat recharge. *Geophys. Res. Lett.* **45**, 3274–3284 (2018).
94. Mayer, M. & Balmaseda, M. A. Indian Ocean impact on ENSO evolution 2014–2016 in a set of seasonal forecasting experiments. *Clim. Dyn.* **56**, 2631–2649 (2021).
95. Nonaka, M., Xie, S.-P. & McCreary, J. P. Decadal variations in the subtropical cells and equatorial pacific SST. *Geophys. Res. Lett.* **29**, 20-1–20-4 (2002).
96. Graffino, G., Farneti, R., Kucharski, F. & Molteni, F. The effect of wind stress anomalies and location in driving Pacific subtropical cells and tropical climate. *J. Clim.* **32**, 1641–1660 (2019).
97. Zhang, H., Clement, A. & Di Nezio, P. The South Pacific Meridional Mode: a mechanism for ENSO-like variability. *J. Clim.* **27**, 769–783 (2014).
98. Chiang, J. C. H. & Vimont, D. J. Analogous Pacific and Atlantic meridional modes of tropical atmosphere–ocean variability. *J. Clim.* **17**, 4143–4158 (2004).
99. Xie, S.-P. & Philander, S. G. H. A coupled ocean–atmosphere model of relevance to the ITCZ in the eastern Pacific. *Tellus A* **46**, 340–350 (1994).
100. Amaya, D. J. et al. The North Pacific pacemaker effect on historical ENSO and its mechanisms. *J. Clim.* **32**, 7643–7661 (2019).
101. Anderson, B. T., Perez, R. C. & Karspeck, A. Triggering of El Niño onset through trade wind-induced charging of the equatorial Pacific. *Geophys. Res. Lett.* **40**, 1212–1216 (2013).
102. Chakravorty, S. et al. Ocean dynamics are key to extratropical forcing of El Niño. *J. Clim.* **34**, 8739–8753 (2021).
103. Hu, R., Lian, T., Feng, J. & Chen, D. Pacific meridional mode does not induce strong positive SST anomalies in the central Equatorial Pacific. *J. Clim.* **36**, 4113–4131 (2023).
104. Vimont, D. J., Alexander, M. A. & Newman, M. Optimal growth of central and East Pacific ENSO events. *Geophys. Res. Lett.* **41**, 4027–4034 (2014).
105. Capotondi, A. & Sardeshmukh, P. D. Optimal precursors of different types of ENSO events. *Geophys. Res. Lett.* **42**, 9952–9960 (2015).
106. Capotondi, A. & Ricciardulli, L. The influence of Pacific winds on ENSO diversity. *Sci. Rep.* **11**, 18672 (2021).
107. Di Lorenzo, E. et al. ENSO and meridional modes: a null hypothesis for Pacific climate variability. *Geophys. Res. Lett.* **42**, 9440–9448 (2015).
108. Okumura, Y. M. Origins of tropical Pacific decadal variability: role of stochastic atmospheric forcing from the South Pacific. *J. Clim.* **26**, 9791–9796 (2013).
109. Zhao, Y. & Di Lorenzo, E. The impacts of extra-tropical ENSO precursors on tropical Pacific decadal-scale variability. *Sci. Rep.* **10**, 3031 (2020).
110. Stuecker, M. F. Revisiting the Pacific meridional mode. *Sci. Rep.* **8**, 3216 (2018).
111. Sanchez, S. C., Amaya, D. J., Miller, A. J., Xie, S.-P. & Charles, C. D. The Pacific meridional mode over the last millennium. *Clim. Dyn.* **53**, 3547–3560 (2019).
112. McGregor, S., Holbrook, N. J. & Power, S. B. The response of a stochastically forced ENSO model to observed off-equatorial wind stress forcing. *J. Clim.* **22**, 2512–2525 (2009).
113. Liguori, G. & Di Lorenzo, E. Separating the North and South Pacific meridional modes contributions to ENSO and tropical decadal variability. *Geophys. Res. Lett.* **46**, 906–915 (2019).
114. Chung, C. T. Y., Power, S. B., Sullivan, A. & Delage, F. The role of the South Pacific in modulating tropical Pacific variability. *Sci. Rep.* **9**, 18311 (2019).
115. Sun, T. & Okumura, Y. M. Role of stochastic atmospheric forcing from the South and North Pacific in tropical Pacific decadal variability. *J. Clim.* **32**, 4013–4038 (2019).
116. Lou, J., Holbrook, N. J. & O'Kane, T. J. South Pacific decadal climate variability and potential predictability. *J. Clim.* **32**, 6051–6069 (2019).
117. Newman, M. et al. The Pacific decadal oscillation, revisited. *J. Clim.* **29**, 4399–4427 (2016).
118. Capotondi, A., Newman, M., Xu, T. & Di Lorenzo, E. An optimal precursor of Northeast Pacific marine heatwaves and central Pacific El Niño events. *Geophys. Res. Lett.* **49**, e2021GL097350 (2022).
119. Lorenzo, E. D. et al. Modes and mechanisms of Pacific decadal-scale variability. *Annu. Rev. Mar. Sci.* **15**, 249–275 (2023).
120. Zhang, Y. et al. Atmospheric forcing of the Pacific meridional mode: tropical Pacific-driven versus internal variability. *Geophys. Res. Lett.* **49**, e2022GL098148 (2022).
121. Stuecker, M. F. et al. Strong remote control of future equatorial warming by off-equatorial forcing. *Nat. Clim. Change* **10**, 124–129 (2020).
122. Hazeleger, W., Severijns, C., Seager, R. & Molteni, F. Tropical Pacific-driven decadal energy transport variability. *J. Clim.* **18**, 2037–2051 (2005).
123. Farneti, R., Molteni, F. & Kucharski, F. Pacific interdecadal variability driven by tropical–extratropical interactions. *Clim. Dyn.* **42**, 3337–3355 (2014).
124. Cai, W. et al. Pantropical climate interactions. *Science* **363**, eaav4236 (2019).
125. Gill, A. E. Some simple solutions for heat-induced tropical circulation. *Q. J. R. Meteorol. Soc.* **106**, 447–462 (1980).
126. Mochizuki, T., Kimoto, M., Watanabe, M., Chikamoto, Y. & Ishii, M. Interbasin effects of the Indian Ocean on Pacific decadal climate change. *Geophys. Res. Lett.* **43**, 7168–7175 (2016).
127. Kucharski, F. et al. The teleconnection of the tropical Atlantic to Indo-Pacific Sea surface temperatures on inter-annual to centennial time scales: a review of recent findings. *Atmosphere* **7**, 29 (2016).
128. Li, X., Xie, S.-P., Gille, S. T. & Yoo, C. Atlantic-induced pan-tropical climate change over the past three decades. *Nat. Clim. Change* **6**, 275–279 (2016).
129. Ruprich-Robert, Y. et al. Assessing the climate impacts of the observed Atlantic multidecadal variability using the GFDL CM2.1 and NCAR CESM1 global coupled models. *J. Clim.* **30**, 2785–2810 (2017).
130. Ruprich-Robert, Y. et al. Impacts of Atlantic multidecadal variability on the tropical Pacific: a multi-model study. *npj Clim. Atmos. Sci.* **4**, 33 (2021).
131. Sun, C. et al. Western tropical Pacific multidecadal variability forced by the Atlantic multidecadal oscillation. *Nat. Commun.* **8**, 15998 (2017).
132. Johnson, Z. F., Chikamoto, Y., Wang, S. Y. S., McPhaden, M. J. & Mochizuki, T. Pacific decadal oscillation remotely forced by the equatorial Pacific and the Atlantic Oceans. *Clim. Dyn.* **55**, 789–811 (2020).
133. Xie, S.-P., Okumura, Y., Miyama, T. & Timmermann, A. Influences of Atlantic climate change on the tropical Pacific via the central American isthmus. *J. Clim.* **21**, 3914–3928 (2008).
134. Orihuela-Pinto, B., England, M. H. & Taschetto, A. S. Interbasin and interhemispheric impacts of a collapsed Atlantic overturning circulation. *Nat. Clim. Change* **12**, 558–565 (2022).
135. Ham, Y.-G., Kug, J.-S., Park, J.-Y. & Jin, F.-F. Sea surface temperature in the north tropical Atlantic as a trigger for El Niño/Southern Oscillation events. *Nat. Geosci.* **6**, 112–116 (2013).
136. Dhame, S., Taschetto, A. S., Santoso, A. & Meissner, K. J. Indian Ocean warming modulates global atmospheric circulation trends. *Clim. Dyn.* **55**, 2053–2073 (2020).
137. Polo, I., Martin-Rey, M., Rodriguez-Fonseca, B., Kucharski, F. & Mechoso, C. R. Processes in the Pacific La Niña onset triggered by the Atlantic Niño. *Clim. Dyn.* **44**, 115–131 (2015).
138. Kucharski, F. et al. Atlantic forcing of Pacific decadal variability. *Clim. Dyn.* **46**, 2337–2351 (2016).
139. Chikamoto, Y., Mochizuki, T., Timmermann, A., Kimoto, M. & Watanabe, M. Potential tropical Atlantic impacts on Pacific decadal climate trends. *Geophys. Res. Lett.* **43**, 7143–7151 (2016).
140. Chikamoto, Y. et al. Skilful multi-year predictions of tropical trans-basin climate variability. *Nat. Commun.* **6**, 6869 (2015).
141. Sobel, A. H., Nilsson, J. & Polvani, L. M. The weak temperature gradient approximation and balanced tropical moisture waves. *J. Atmos. Sci.* **58**, 3650–3665 (2001).
142. Bretherton, C. S. & Sobel, A. H. The Gill model and the weak temperature gradient approximation. *J. Atmos. Sci.* **60**, 451–460 (2003).
143. Chiang, J. C. H. & Sobel, A. H. Tropical tropospheric temperature variations caused by ENSO and their influence on the remote tropical climate. *J. Clim.* **15**, 2616–2631 (2002).
144. Bjerknes, J. Atmospheric teleconnections from the equatorial Pacific. *Mon. Weather Rev.* **97**, 163–172 (1969).
145. Naha, R., McGregor, S. & Singh, M. Exploring the symmetries of pantropical connections between the tropical Atlantic and Pacific basins. *J. Clim.* **36**, 5251–5265 (2023).
146. Kajtar, J. B., Santoso, A., England, M. H. & Cai, W. Tropical climate variability: interactions across the Pacific, Indian, and Atlantic Oceans. *Clim. Dyn.* **48**, 2173–2190 (2017).

147. Terray, P., Masson, S., Prodhomme, C., Roxy, M. K. & Sooraj, K. P. Impacts of Indian and Atlantic oceans on ENSO in a comprehensive modeling framework. *Clim. Dyn.* **46**, 2507–2533 (2016).
148. Meehl, G. A. et al. Atlantic and Pacific tropics connected by mutually interactive decadal-timescale processes. *Nat. Geosci.* **14**, 36–42 (2021).
149. O'Reilly, C. H. et al. Challenges with interpreting the impact of Atlantic multidecadal variability using SST-restoring experiments. *npj Clim. Atmos. Sci.* **6**, 14 (2023).
150. Penland, C. & Sardeshmukh, P. D. The optimal-growth of tropical sea-surface temperature anomalies. *J. Clim.* **8**, 1999–2024 (1995).
151. Zhao, Y., Newman, M., Capotondi, A., Di Lorenzo, E. & Sun, D. Removing the effects of tropical dynamics from North Pacific climate variability. *J. Clim.* **34**, 9249–9265 (2021).
152. Zhao, Y., Jin, Y., Li, J. & Capotondi, A. The role of extratropical Pacific in crossing ENSO spring predictability barrier. *Geophys. Res. Lett.* **49**, e2022GL099488 (2022).
153. Zhao, Y., Jin, Y., Capotondi, A., Li, J. & Sun, D. The role of tropical Atlantic in ENSO predictability barrier. *Geophys. Res. Lett.* **50**, e2022GL101853 (2023).
154. Qiu, B. & Chen, S. Interannual-to-decadal variability in the bifurcation of the North equatorial current off the Philippines. *J. Phys. Oceanogr.* **40**, 2525–2538 (2010).
155. Capotondi, A., Alexander, M. A., Bond, N. A., Curchitser, E. N. & Scott, J. D. Enhanced upper ocean stratification with climate change in the CMIP3 models. *J. Geophys. Res. Ocean.* **117**, C04031 (2012).
156. Geng, T., Yang, Y. & Wu, L. On the mechanisms of Pacific decadal oscillation modulation in a warming climate. *J. Clim.* **32**, 1443–1459 (2019).
157. Xu, Y. & Hu, A. How would the twenty-first-century warming influence Pacific decadal variability and its connection to North American rainfall: assessment based on a revised procedure for the IPO/PDO. *J. Clim.* **31**, 1547–1563 (2018).
158. Jia, F. et al. Weakening Atlantic Niño–Pacific connection under greenhouse warming. *Sci. Adv.* **5**, eaax4111 (2019).
159. Jia, F., Cai, W., Gan, B., Wu, L. & Di Lorenzo, E. Enhanced North Pacific impact on El Niño/Southern Oscillation under greenhouse warming. *Nat. Clim. Change* **11**, 840–847 (2021).
160. Liguori, G. & Di Lorenzo, E. Meridional modes and increasing Pacific decadal variability under anthropogenic forcing. *Geophys. Res. Lett.* **45**, 983–991 (2018).
161. Huang, B. Y. et al. Extended reconstructed sea surface temperature, version 5 (ERSSTv5): upgrades, validations, and intercomparisons. *J. Clim.* **30**, 8179–8205 (2017).
162. Kalnay, E. et al. The NCEP/NCAR 40-year reanalysis project. *Bull. Am. Meteorol. Soc.* **77**, 437–472 (1996).
163. Zuo, H., Balmaseda, M. A., Tietsche, S., Mogensen, K. & Mayer, M. The ECMWF operational ensemble reanalysis–analysis system for ocean and sea ice: a description of the system and assessment. *Ocean Sci.* **15**, 779–808 (2019).
164. Balmaseda, M. A., Mogensen, K. & Weaver, A. T. Evaluation of the ECMWF ocean reanalysis system ORAS4. *Q. J. Roy. Meteor. Soc.* **139**, 1132–1161 (2013).
165. Behringer, D. & Xue, Y. in *Eighth Symposium on Integrated Observing and Assimilation Systems for Atmosphere, Oceans, and Land Surface* (AMS, 2004).
166. Carton, J. A. & Giese, B. S. A reanalysis of ocean climate using Simple Ocean Data Assimilation (SODA). *Mon. Weather Rev.* **136**, 2999–3017 (2008).
167. Zuo, H., Balmaseda, M. A. & Mogensen, K. The new eddy-permitting ORAP5 ocean reanalysis: description, evaluation and uncertainties in climate signals. *Clim. Dyn.* **49**, 791–811 (2017).
168. You, Y. & Furtado, J. C. The South Pacific meridional mode and its role in tropical Pacific climate variability. *J. Clim.* **31**, 10141–10163 (2018).
169. Naha, R., McGregor, S. & Singh, M. Exploring the asymmetries of pan-tropical connections from the tropical Indian to the Pacific basin. *J. Clim.* https://doi.org/10.1175/JCLI-D-22-0845.1 (2023).
170. Hu, D. et al. Pacific western boundary currents and their roles in climate. *Nature* **522**, 299–308 (2015).
171. Cobb, K. M., Charles, C. D., Cheng, H. & Edwards, R. L. El Niño/Southern Oscillation and tropical Pacific climate during the last millennium. *Nature* **424**, 271–276 (2003).
172. Ramos, R. D., Goodkin, N. F., Siringan, F. P. & Hughen, K. A. Coral records of temperature and salinity in the tropical Western Pacific reveal influence of the Pacific decadal oscillation since the late nineteenth century. *Paleoceanogr. Paleoclimatol.* **34**, 1344–1358 (2019).
173. Nurhati, I. S., Cobb, K. M. & Di Lorenzo, E. Decadal-scale SST and salinity variations in the central tropical Pacific: signatures of natural and anthropogenic climate change. *J. Clim.* **24**, 3294–3308 (2011).
174. Sanchez, S. C., Charles, C. D., Carriquiry, J. D. & Villaescusa, J. A. Two centuries of coherent decadal climate variability across the Pacific North American region. *Geophys. Res. Lett.* **43**, 9208–9216 (2016).
175. Dassié, E. P., Hasson, A., Khodri, M., Lebas, N. & Linsley, B. K. Spatiotemporal variability of the South Pacific convergence zone fresh pool eastern front from coral-derived surface salinity data. *J. Clim.* **31**, 3265–3288 (2018).
176. Thompson, D. M., Cole, J. E., Shen, G. T., Tudhope, A. W. & Meehl, G. A. Early twentieth-century warming linked to tropical Pacific wind strength. *Nat. Geosci.* **8**, 117–121 (2015).
177. Guilderson, T. P. & Schrag, D. P. Abrupt shift in subsurface temperatures in the tropical Pacific associated with changes in El Nino. *Science* **281**, 240–243 (1998).
178. Druffel, E. R. M. et al. Seasonal radiocarbon and oxygen isotopes in a Galapagos coral: calibration with climate indices. *Geophys. Res. Lett.* **41**, 5099–5105 (2014).
179. Abram, N. J. et al. Coupling of Indo-Pacific climate variability over the last millennium. *Nature* **579**, 385–392 (2020).
180. Cobb, K. M., Charles, C. D. & Hunter, D. E. A central tropical Pacific coral demonstrates Pacific, Indian, and Atlantic decadal climate connections. *Geophys. Res. Lett.* **28**, 2209–2212 (2001).
181. Huang, B. et al. Extended reconstructed sea surface temperature version 4 (ERSST.v4). Part I: upgrades and intercomparisons. *J. Clim.* **28**, 911–930 (2015).
182. Hirahara, S., Ishii, M. & Fukuda, Y. Centennial-scale sea surface temperature analysis and its uncertainty. *J. Clim.* **27**, 57–75 (2014).
183. Rayner, N. A. et al. Global analyses of sea surface temperature sea ice and night marine air temperature since the late nineteenth century. *J. Geophys. Res.* **108**, 4407 (2003).
184. Kaplan, A. et al. Analyses of global sea surface temperature 1856–1991. *J. Geophys. Res.* **103**, 18567–18589 (1998).
185. Taylor, K. E., Stouffer, R. J. & Meehl, G. A. An overview of CMIP5 and the experiment design. *Bull. Amer. Meteor. Soc.* **93**, 485–498 (2012).
186. Eyring, V. et al. Overview of the Coupled Model Intercomparison Project Phase 6 (CMIP6) experimental design and organization. *Geosci. Model Dev.* **9**, 1937–1958 (2016).
187. Braconnot, P. et al. Evaluation of climate models using palaeoclimatic data. *Nat. Clim. Change* **2**, 417–424 (2012).
188. Otto-Bliesner, B. L. et al. Climate variability and change since 850 CE: an ensemble approach with the community earth system model. *Bull. Amer. Meteor. Soc.* **97**, 735–754 (2016).
189. Cobb, K. M. et al. Highly variable El Niño–Southern Oscillation throughout the Holocene. *Science* **339**, 67–70 (2013).
190. Dunbar, R. B., Wellington, G. M., Colgan, M. W. & Glynn, P. W. Eastern Pacific sea surface temperature since 1600 A.D.: the $\delta^{18}O$ record of climate variability in Galápagos corals. *Paleoceanography* **9**, 291–315 (1994).
191. Sanchez, S. C. et al. A continuous record of central tropical Pacific climate since the midnineteenth century reconstructed from Fanning and Palmyra Island corals: a case study in coral data reanalysis. *Paleoceanogr. Paleoclimatol.* **35**, e2020PA003848 (2020).
192. Emile-Geay, J., Cobb, K. M., Mann, M. E. & Wittenberg, A. T. Estimating central equatorial Pacific SST variability over the past millennium. Part II: reconstructions and implications. *J. Clim.* **26**, 2329–2352 (2013).
193. Li, J. et al. El Niño modulations over the past seven centuries. *Nat. Clim. Change* **3**, 822–826 (2013).
194. Hakim, G. J. et al. The last millennium climate reanalysis project: framework and first results. *J. Geophys. Res. Atmos.* **121**, 6745–6764 (2016).
195. Steiger, N. J., Smerdon, J. E., Cook, E. R. & Cook, B. I. A reconstruction of global hydroclimate and dynamical variables over the common era. *Sci. Data* **5**, 180086 (2018).
196. Bechtold, B. Violin plots for Matlab, GitHub project. *GitHub* https://github.com/bastibe/Violinplot-Matlab (2016).

Acknowledgements

This paper is a product of the CLIVAR Pacific Region Panel working group on 'Tropical Pacific Decadal Variability'. The authors thank CLIVAR for their sponsorship and J. Li at the CLIVAR Program Office for her help. The paper was finalized during a workshop held at Monash University, Australia. The authors acknowledge workshop funding support from the Faculty of Science and the School of Earth Atmosphere and Environment at Monash University, as well as CLIVAR and US CLIVAR. The authors also thank N. Renier from the Woods Hole Oceanographic Institution graphics team for her help in the preparation of the figure in Box 1. A.C. was supported by the NOAA Climate Program Office's Climate Variability and Predictability (CVP) and Modeling, Analysis, Predictions and Projections (MAPP) programmes and by DOE Award No. DE-SC0023228. S.M. was supported by the Australian Research Council (grant numbers FT160100162 and DP200102329) and the Australian Government's National Environmental Science Program (NESP2) Climate Systems Hub. S.C. was supported by IRD (French National Research Institute for Sustainable Development). M.F.S. was supported by NSF grant AGS-2141728 and NOAA's Climate Program Office's MAPP programme grant NA20OAR4310445. This is IPRC publication 1611 and SOEST contribution 11719. J.S. was supported by NOAA's Global Ocean Monitoring and Observing Program (Award NA20OAR4320278). Y.I. and Y.K. were supported by the Program for Advanced Studies of Climate Change Projection (SENTAN, JPMXD0722680395) from the Ministry of Education, Culture, Sports, Science and Technology, Japan. A.S is supported by Australian Government's NESP and was supported by the Centre for Southern Hemisphere Oceans Research. K.B.K. was supported by the NASA Sea Level Change Science Program, Award 80NSSC20K1123. N.J.H. and A.S.T. were supported by funding from the ARC Centre of Excellence for Climate Extremes (grant number CE170100023) and acknowledge support from the NESP2 Climate Systems Hub. M.M. was supported by the Austrian Science Fund project P33177. S.S. was supported by the US Department of Energy, DE-SC0019418 and the US National Science Foundation (NSF), OCE-2202794 and AGS-1805143. C.M.-V. was supported by Proyecto ANID Fondecyt 3200621. R.M.H. was supported by the Australian Research Council through grant number DE21010004. C.C.U. was supported by NSF award AGS-2002083 and the James E. and Barbara V. Moltz Fellowship for Climate-Related Research. G.A.M. was supported by the Regional and Global Model Analysis component of the Earth and Environmental System Modelling Program of the US Department of Energy's Office of Biological and Environmental Research under Award Number DE-SC0022070 and also by the National Center for Atmospheric Research, which is a major facility sponsored by the NSF under Cooperative Agreement No. 1852977. N.S. acknowledges support from the joint JAMSTEC-IPRC Collaborative Research project JICore and from the US Office of Naval Research through the Climate Resilience Collaborative at the University of Hawai'i at Mānoa. M.J.M. was supported by NOAA. This is PMEL contribution no. 5499.

Author contributions

A.C. and S.M. conceived the Review. A.C., S.M., M.J.M., S.C., N.J.H., Y.I., S.C.S., J.S., M.F.S. and M.Z. coordinated the writing of the various sections. A.C., S.M., C.C.U. and S.C.S led the analyses and the preparation of the figures. All authors contributed to the discussion and interpretation of the material and assisted with the writing of the manuscript, led by A.C.

Competing interests

The authors declare no competing interests.

Additional information

Peer review information *Nature Reviews Earth & Environment* thanks Xiaopei Lin, Masami Nonaka, Xichen Li and the other, anonymous, reviewer(s) for their contribution to the peer review of this work.

[1]Cooperative Institute for Research in Environmental Sciences, University of Colorado Boulder, Boulder, CO, USA. [2]NOAA/Physical Sciences Laboratory, Boulder, CO, USA. [3]School of Earth Atmosphere and Environment, Monash University, Clayton, Victoria, Australia. [4]ARC Centre of Excellence for Climate Extremes, Monash University, Clayton, Victoria, Australia. [5]NOAA/Pacific Marine Environmental Laboratory, Seattle, WA, USA. [6]LEGOS, Université de Toulouse, IRD, CNES, CNRS, UPS, Toulouse, France. [7]IRD, Nouméa, New Caledonia. [8]Institute for Marine and Antarctic Studies, University of Tasmania, Hobart, Tasmania, Australia. [9]ARC Centre of Excellence for Climate Extremes, University of Tasmania, Hobart, Tasmania, Australia. [10]Atmosphere and Ocean Research Institute, University of Tokyo, Chiba, Japan. [11]Department of Atmospheric and Oceanic Sciences, University of Colorado Boulder, Boulder, CO, USA. [12]Scripps Institution of Oceanography, University of California San Diego, La Jolla, CA, USA. [13]Department of Oceanography, School of Ocean and Earth Science and Technology (SOEST), University of Hawai'i at Mānoa, Honolulu, HI, USA. [14]International Pacific Research Center (IPRC), School of Ocean and Earth Science and Technology (SOEST), University of Hawai'i at Mānoa, Honolulu, HI, USA. [15]Department of Physical Oceanography, Woods Hole Oceanographic Institution, Woods Hole, MA, USA. [16]ARC Centre of Excellence for Climate Extremes, University of New South Wales, Sydney, New South Wales, Australia. [17]GEOMAR Helmholtz Centre for Ocean Research, Kiel, Germany. [18]Abdus Salam International Centre for Theoretical Physics, Trieste, Italy. [19]National Centre for Atmospheric Science, Department of Meteorology, University of Reading, Reading, UK. [20]CAS Key Laboratory of Ocean Circulation and Waves, Institute of Oceanology, Chinese Academy of Sciences, Qingdao, China. [21]Research Center for Advanced Science and Technology, University of Tokyo, Tokyo, Japan. [22]Research Department, European Centre for Medium-Range Weather Forecasts, Reading, UK. [23]Department of Meteorology and Geophysics, University of Vienna, Vienna, Austria. [24]Climate Change Research Centre, University of New South Wales, Sydney, New South Wales, Australia. [25]Climate Science Centre, CSIRO Environment, Hobart, Tasmania, Australia. [26]School of Geosciences, University of Sydney, Sydney, New South Wales, Australia. [27]Institute of Climate Application Research (ICAR)/CIC-FEMD, Nanjing University of Information Science and Technology, Nanjing, China. [28]Research School of Earth Sciences, Australian National University, Canberra, Australian Capital Territory, Australia. [29]ARC Centre of Excellence for Climate Extremes, Australian National University, Canberra, Australian Capital Territory, Australia. [30]Faculty of Engineering and Science, Universidad Adolfo Ibáñez, Santiago, Chile. [31]Data Observatory Foundation, Santiago, Chile. [32]National Center for Atmospheric Research, Boulder, CO, USA. [33]Bren School of Environmental Science and Management, University of California Santa Barbara, Santa Baranra, CA, USA. [34]CSIRO Oceans and Atmosphere, Aspendale, Victoria, Australia.